Jet fragmentation and multijet studies in heavy ion collisions at ATLAS

Martin Spousta
on behalf of the ATLAS Collaboration

Charles University

Jet studies in heavy ion collisions

- Jet studies in heavy ion collisions at ATLAS:
  - Di-jet asymmetry measurement
  - Inclusive jet suppression – **jet R_{AA}** and R_{CP}
  - Azimuthal dependence of the jet suppression
  - **Jet fragmentation**
  - **Neighboring jet production**
  - Jets and bosons

Main topics of this talk

- Typical configuration of reconstruction:
  - Anti-kt R=0.2, 0.3, 0.4 jets reconstructed in the calorimeter.
  - Data: 2011 Pb+Pb run of 140 μb^{-1}, events triggered using minimum bias trigger or high-level trigger. For some measurements p+p data at 2.76 TeV from 2013.
  - MC: PYTHIA jets embedded to minimum-bias Pb+Pb Data.

Jet studies in heavy ion collisions

- Jet studies in heav… collisions at A…
  - Di-jet asymmetry measurement
  - Inclusive jet suppression – **jet R_{AA}** and R_{CP}
  - Azimuthal dependence of the jet suppression
  - **Jet fragmentation**
  - **Neighboring jet production**
  - Jets and bosons
- Typical configuration of rec…
  - Anti-kt R=0.2, 0.3, 0.4 jets reconstructed in the calorimeter.
  - Data: 2011 Pb+Pb run of 140 μb^{-1}, events triggered using minimum bias trigger or high-level trigger. For some measurements p+p data at 2.76 TeV from 2013.
  - MC: PYTHIA jets embedded to minimum-bias Pb+Pb Data.

PRL 105 (2010) 252303

ATLAS-CONF-2014-025

PLB 719 (2013) 220-241

PRL 111 (2013) 152301

arXiv:1406.2979

Main topics of this talk

ATLAS-CONF-2014-028

ATLAS-CONF-2012-121,
ATLAS-CONF-2012-119

Inclusive jet suppression in Pb+Pb

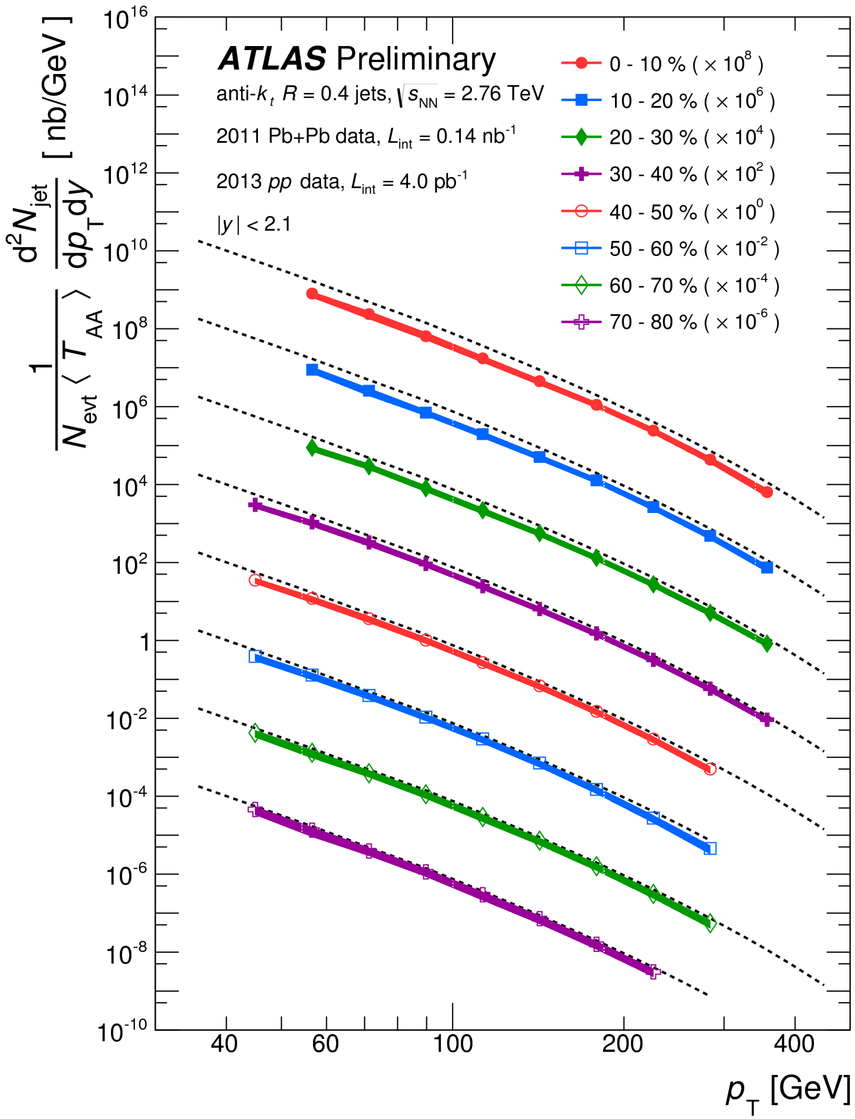

- Jet spectra measured in 8 centrality bins and 5 bins of rapidity within |y|<2.1.
- Spectra used to calculate the nuclear modification factor

$$R_{AA} = \frac{\frac{1}{N_{evnt}} \frac{d^2 N_{jet}^{PbPb}}{dp_T dy}\Big|_{cent}}{\langle T_{AA} \rangle_{cent} \times \frac{d^2 \sigma_{jet}^{pp}}{dp_T dy}}$$

- At different rapidities different steepness of the spectra and different q/g ratio => allows to extract some of the details of the energy loss.

Inclusive jet suppression

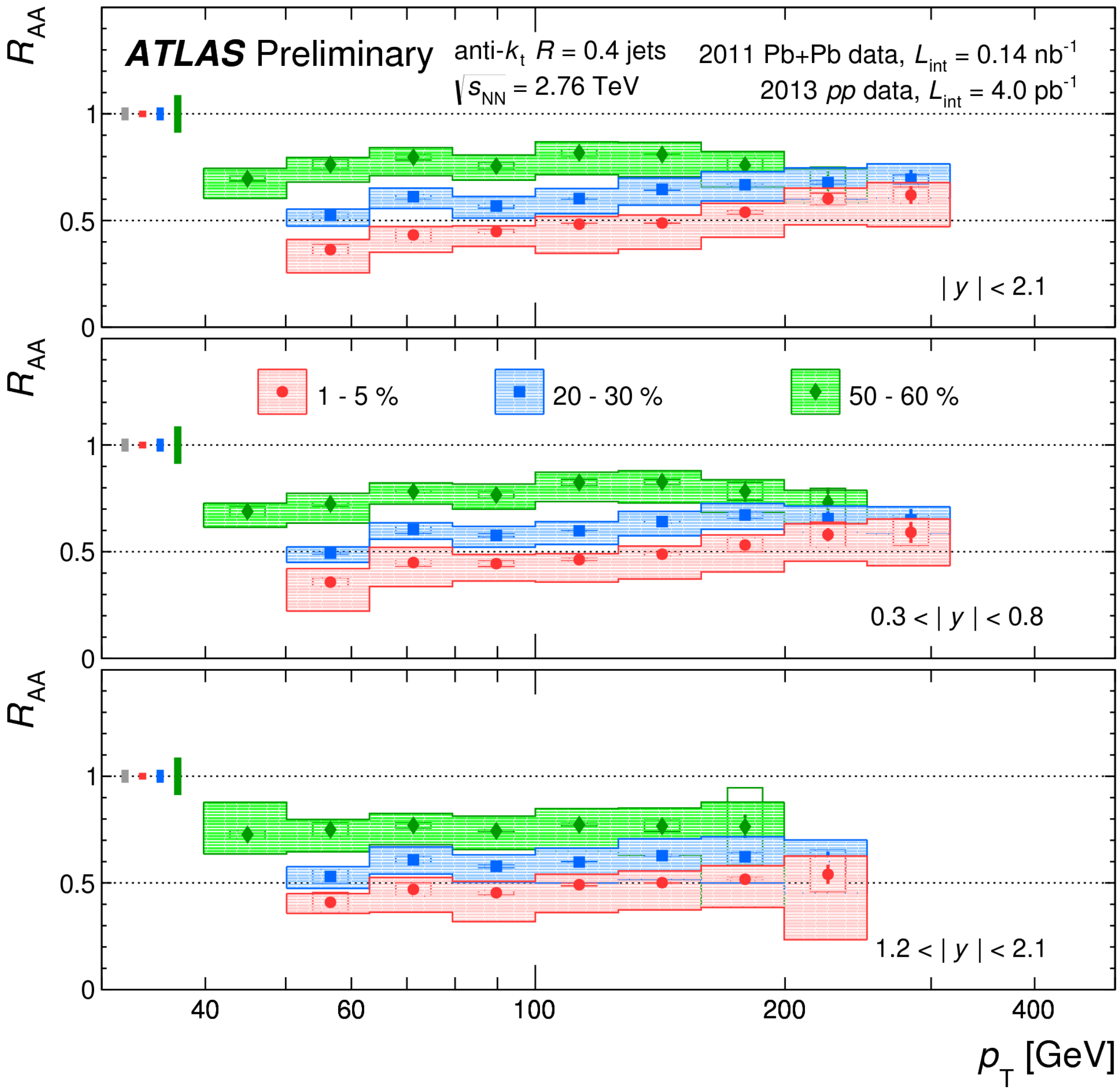

$$R_{AA} = \frac{\frac{1}{N_{evnt}} \left.\frac{d^2 N_{jet}^{PbPb}}{dp_T dy}\right|_{cent}}{\langle T_{AA}\rangle_{cent} \times \frac{d^2\sigma_{jet}^{pp}}{dp_T dy}}$$

- A modest grow of R_{AA} with increasing jet pt.
- Still significant suppression even for 50-60% centrality bin.
- Practically no rapidity dependence.

Jet fragmentation

Jet fragmentation quantities

- Measured quantity #1: Distribution of momentum of fragments inside jets, $D(p_T)$.

$$D(p_{\mathrm{T}})(p_{\mathrm{T}}^{jet}) = \frac{1}{N_{jet}}\frac{1}{\epsilon}\frac{dN}{dp_{\mathrm{T}}}(p_{\mathrm{T}}^{jet}) =$$

$$= \frac{1}{N_{jet}(p_{\mathrm{T}}^{jet})}\frac{1}{\epsilon(p_{\mathrm{T}},\eta)}\left(\frac{\Delta N_{ch}(p_{\mathrm{T}},p_{\mathrm{T}}^{jet})}{\Delta p_{\mathrm{T}}} - \frac{\Delta N_{ch}^{UE}(p_{\mathrm{T}},p_{\mathrm{T}}^{jet})}{\Delta p_{\mathrm{T}}}\right)$$

Tracking efficiency correction

Underlying event subtraction

- Further, the central-to-peripheral ratio of the $D(p_T)$ distribution, $R_{D(pT)}$, is evaluated.

Jet fragmentation quantities

- Measured quantity #2: Distribution of longitudinal momentum fraction of fragments with respect to jet, D(z).

$$D(z)(p_{\mathrm{T}}^{jet}) = \frac{1}{N_{jet}}\frac{1}{\epsilon}\frac{dN}{dz}(p_{\mathrm{T}}^{jet}) =$$

$$= \frac{1}{N_{jet}(p_{\mathrm{T}}^{jet})}\frac{1}{\epsilon(p_{\mathrm{T}},\eta)}\left(\frac{\Delta N_{ch}(z,p_{\mathrm{T}}^{jet})}{\Delta z} - \frac{\Delta N_{ch}^{UE}(z,p_{\mathrm{T}}^{jet})}{\Delta z}\right)$$

$$z = p_{\mathrm{T}}/p_{\mathrm{T}}^{jet}\cos R$$

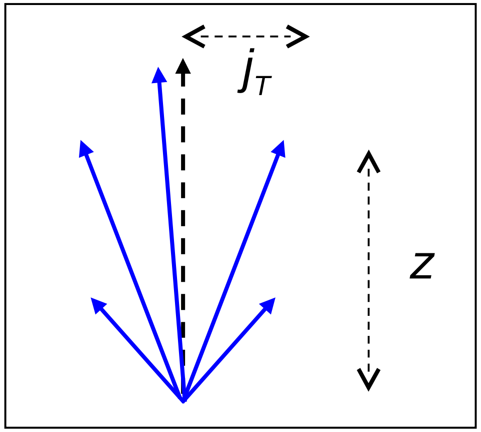

- Further, the central-to-peripheral ratio of the D(z) distribution, $R_{D(z)}$, is evaluated.

Track selection in Pb+Pb

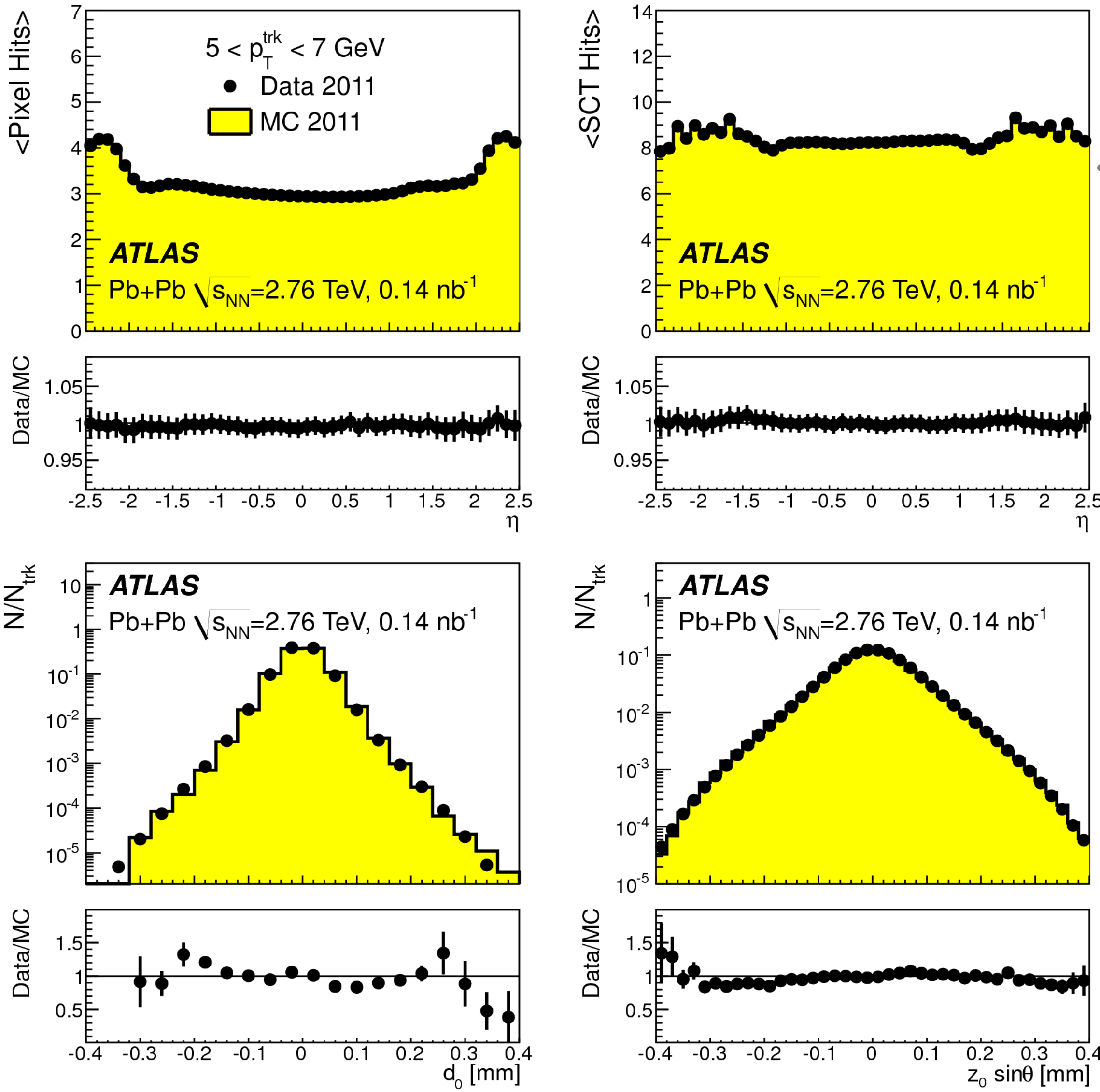

MC to data comparison of tracking performance

- Tracks match to jets using $\Delta R = 0.4$ for all three radii.
- Track selection based on number of hits in Silicon tracker and Pixel detector and significance of pointing to the vertex.
- Tracks with p_T>2 GeV and $|\eta|$<2.5 used => jets reconstructed over $|\eta|$<2.1.

Important experimental corrections

- Contribution from UE to the measured distributions:
  - subtracted jet-by-jet
  - evaluated in each event using a grid of cones
  - each particle in the cone corrected for elliptic flow and difference in eta position
- Tracking efficiency correction:
  - as a function of: centrality, track p_T, and pseudorapidity
- Correction of the jet p_T to reduce the effect of the jet up-feeding due to jet energy resolution.
- Unfolding using SVD method.

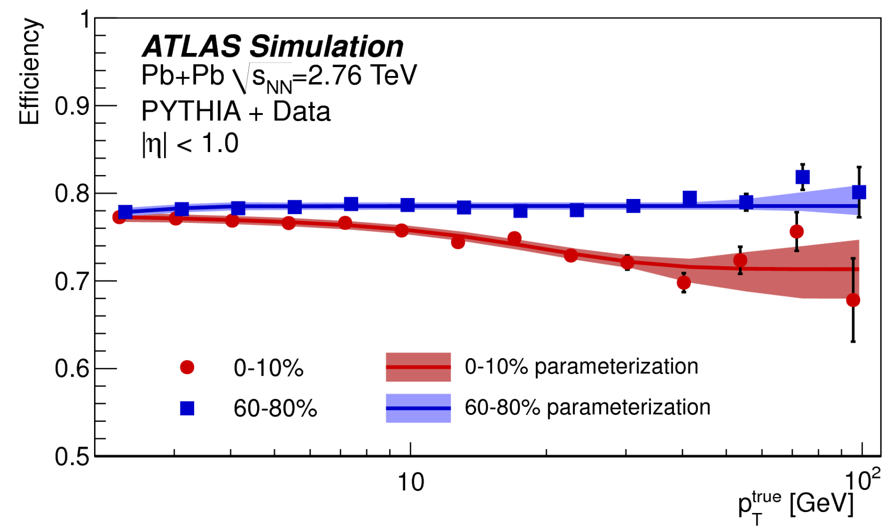

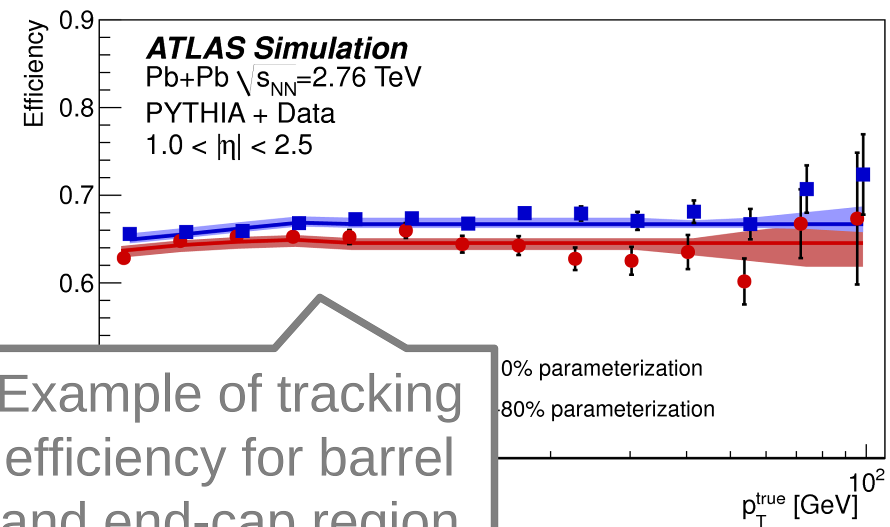

Example of tracking efficiency for barrel and end-cap region

D(z) and D(pt) distributions for R=0.4 jets

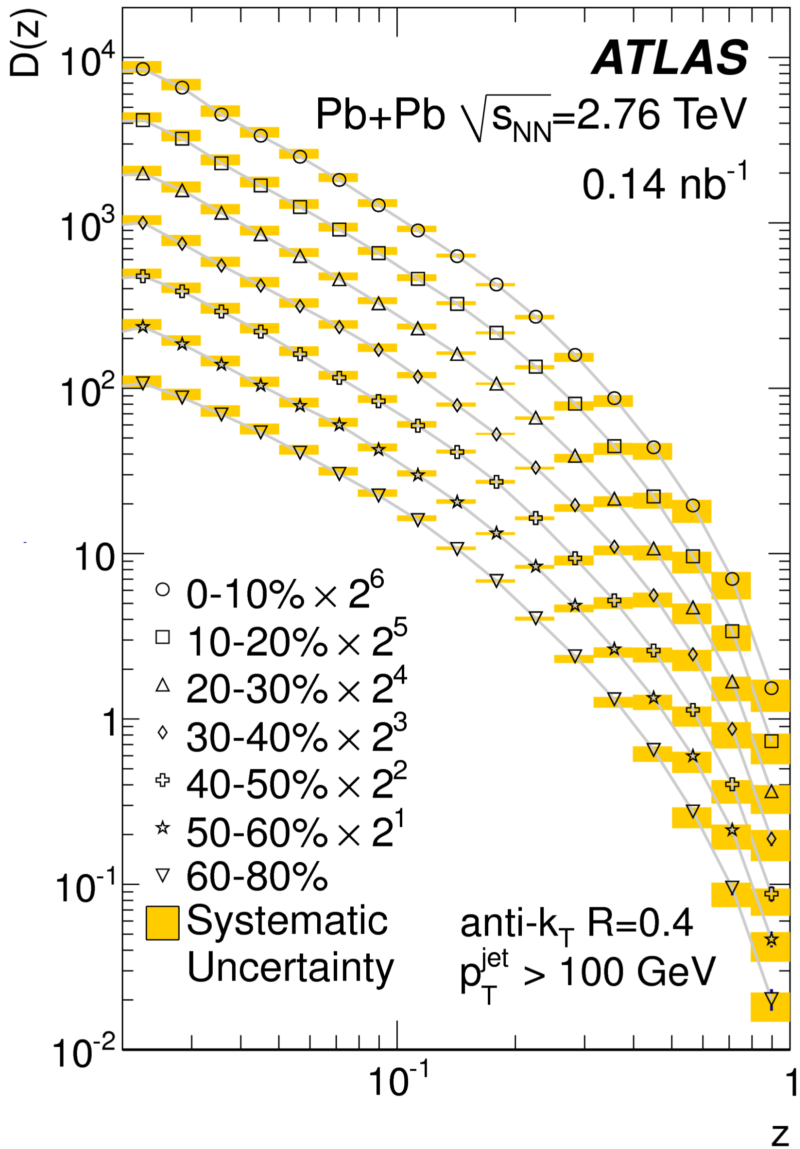

- Fully corrected D(z) distribution for R=0.4 jets.
- Yellow boxes: uncorrelated or partially correlated systematic uncertainties due to:
  - Jet energy scale
  - Jet energy resolution
  - Track reconstruction
  - Unfolding
  - Residual MC non-closure
- Statistical error by error bars (typically invisible).
- Gray line to guide the eye.

D(z) and D(pt) distributions for R=0.4 jets

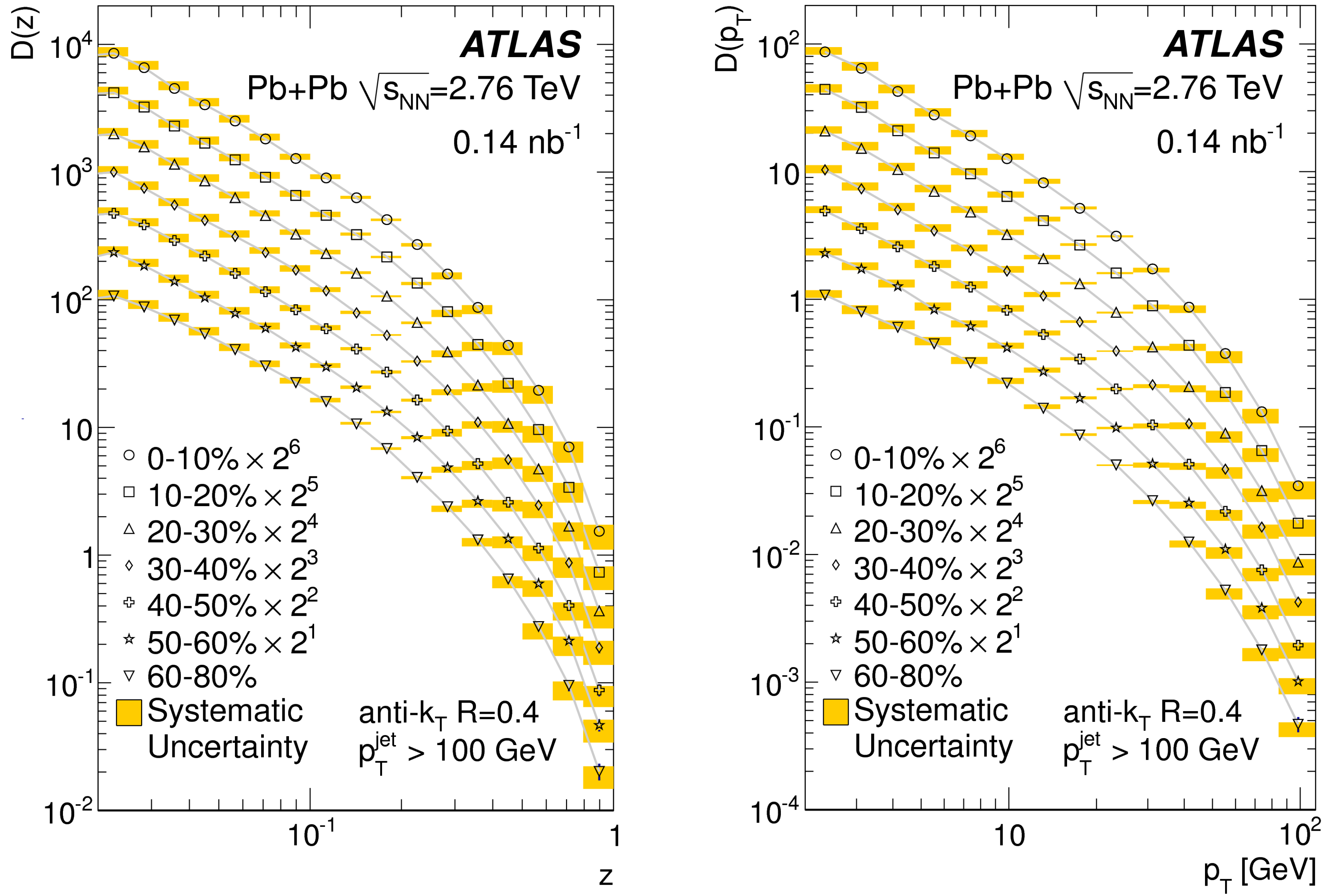

D(z) and D(pt) distributions for R=0.4 jets

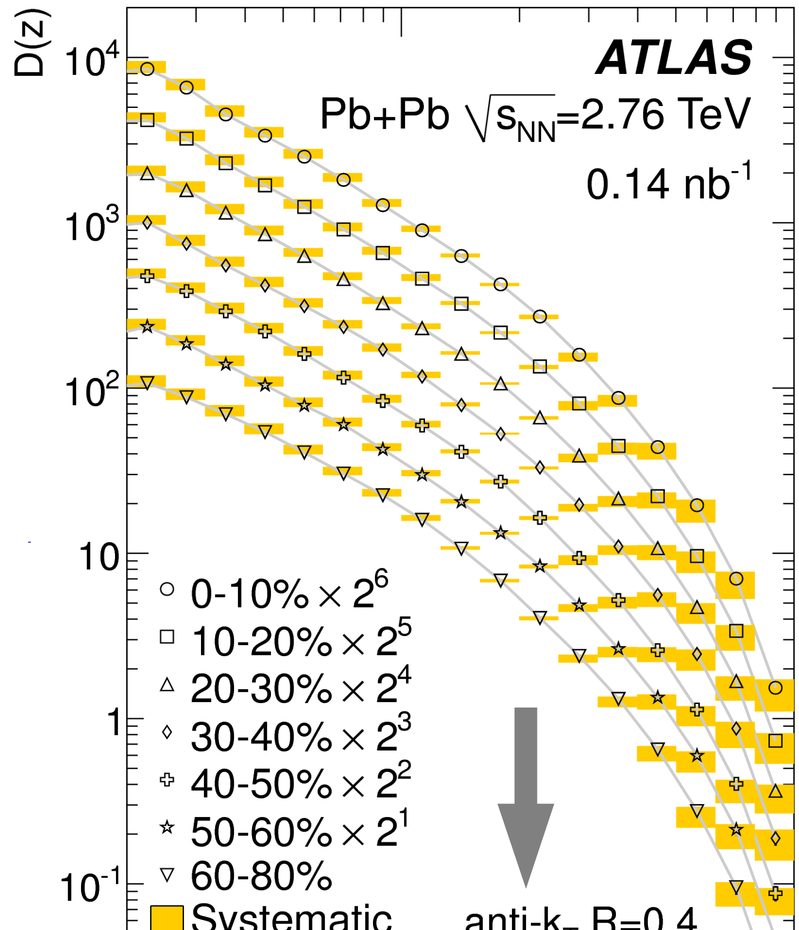

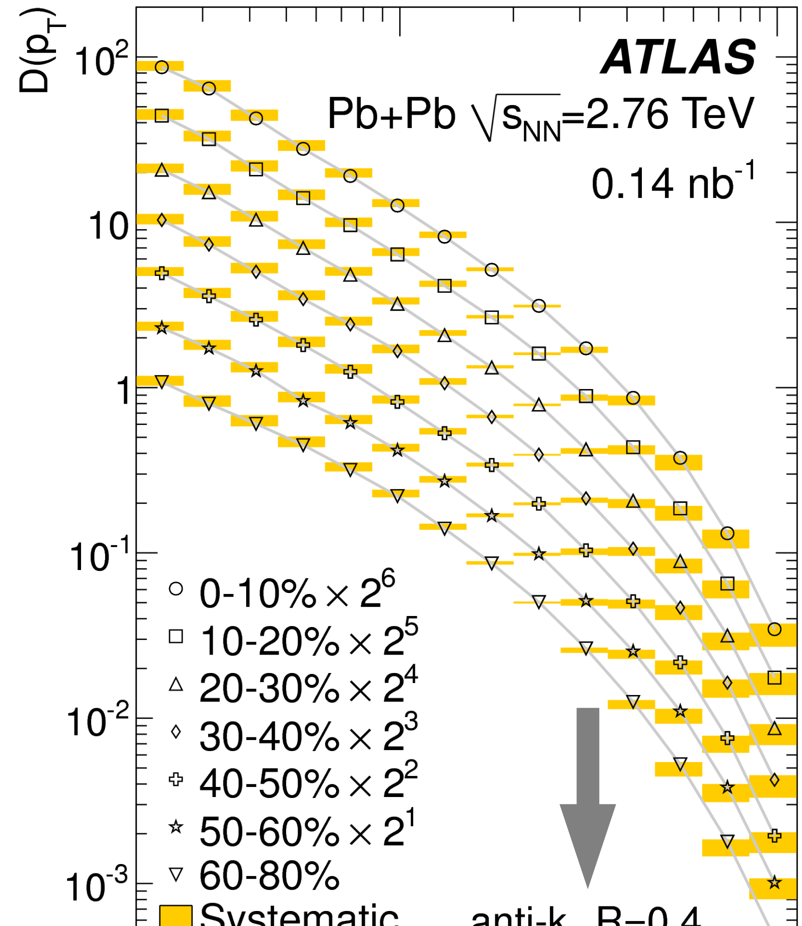

$$R_{\mathrm{D(z)}} = \frac{\mathrm{D}(z)|_{\mathrm{cent}}}{\mathrm{D}(z)|_{60-80\%}}$$

$$R_{\mathrm{D(p_T)}} = \frac{\mathrm{D}(p_T)|_{\mathrm{cent}}}{\mathrm{D}(p_T)|_{60-80\%}}$$

$R_{D(z)}$ and $R_{D(pt)}$

$$R_{\mathrm{D(z)}} = \frac{\mathrm{D}(z)|_{\mathrm{cent}}}{\mathrm{D}(z)|_{60-80\%}}$$

$$R_{\mathrm{D(p_T)}} = \frac{\mathrm{D}(p_T)|_{\mathrm{cent}}}{\mathrm{D}(p_T)|_{60-80\%}}$$

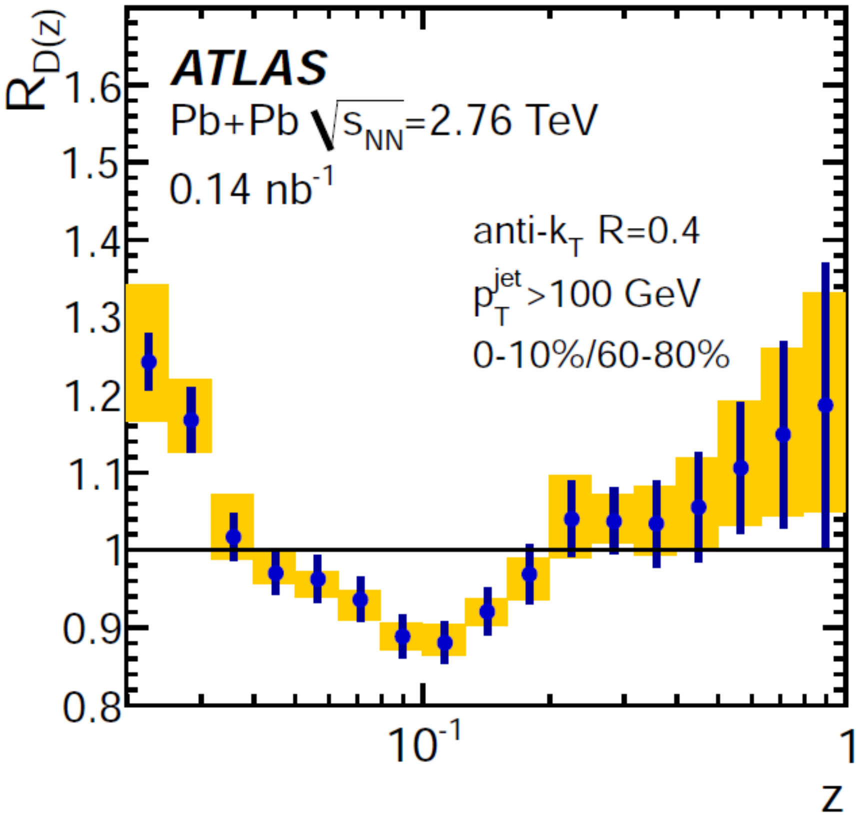

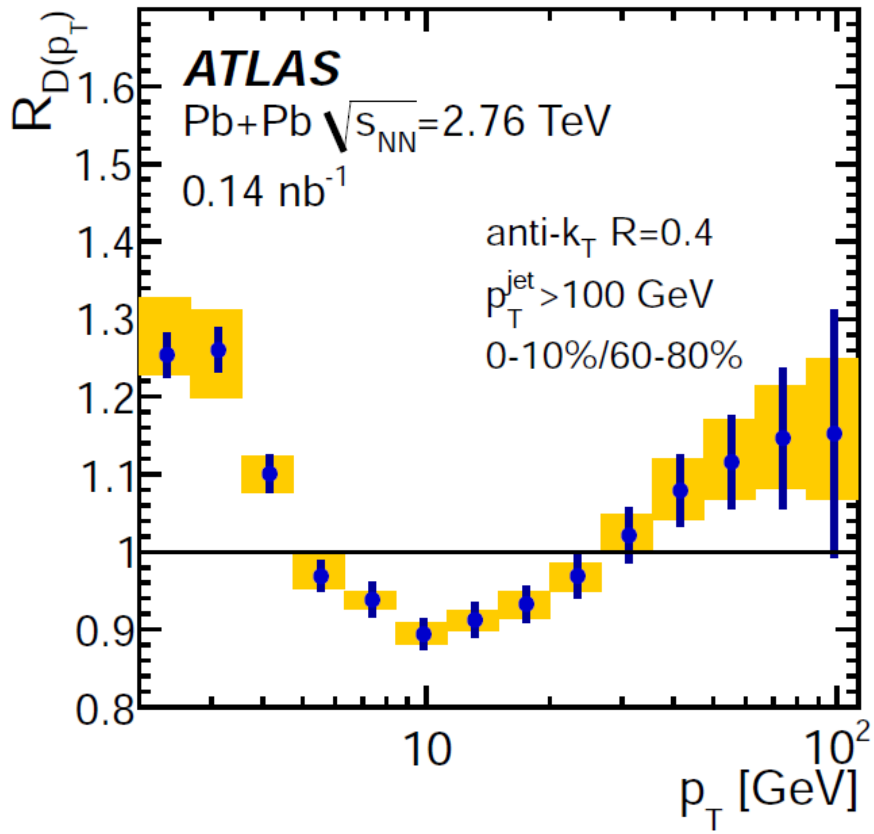

$R_{D(z)}$ and $R_{D(pt)}$

$$R_{\mathrm{D(z)}} = \frac{\mathrm{D}(z)|_{\mathrm{cent}}}{\mathrm{D}(z)|_{60-80\%}}$$

$$R_{\mathrm{D(p_T)}} = \frac{\mathrm{D}(p_T)|_{\mathrm{cent}}}{\mathrm{D}(p_T)|_{60-80\%}}$$

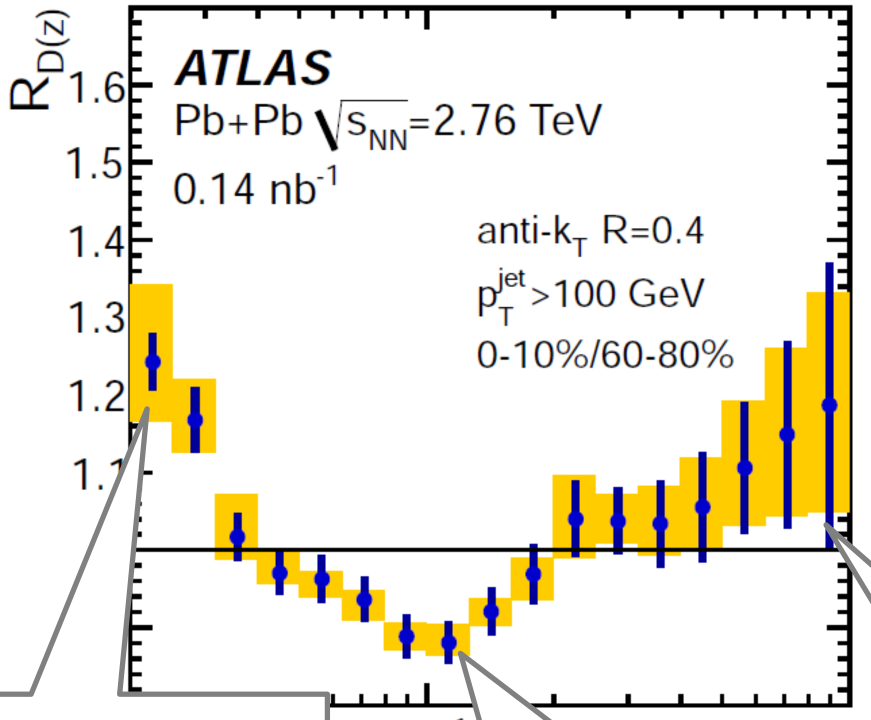

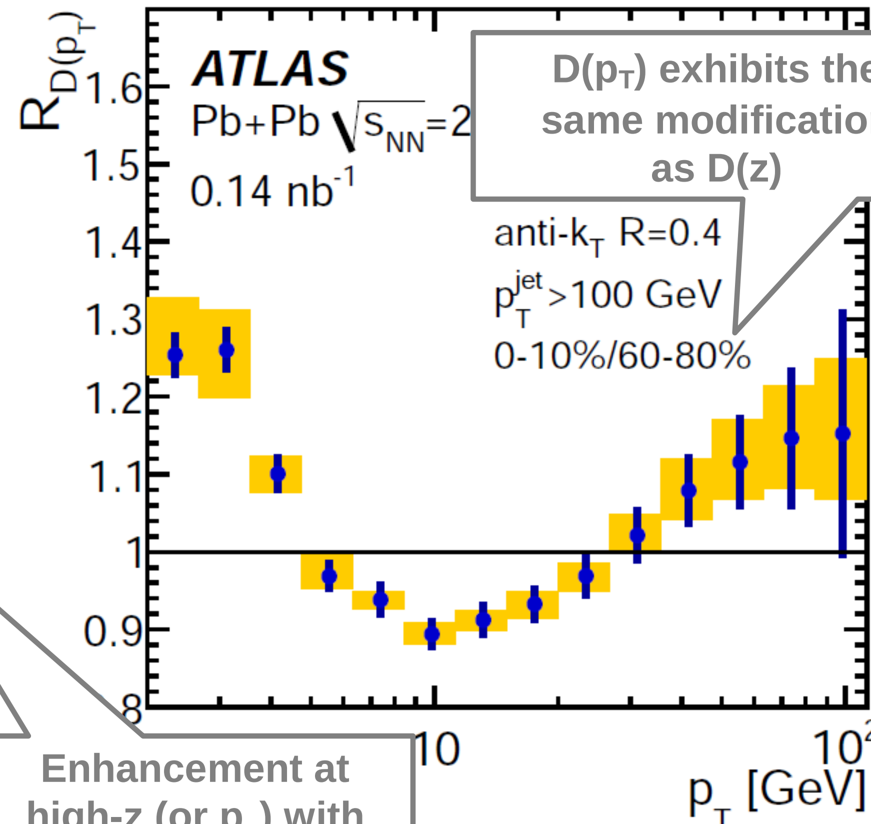

$D(p_T)$ exhibits the same modification as D(z)

Enhancement at low-z (or low- p_T)

Suppression at intermediate-z (or p_T)

Enhancement at high-z (or p_T) with significance of 1-2σ

Full set of $R_{D(z)}$ for R=0.4 jets

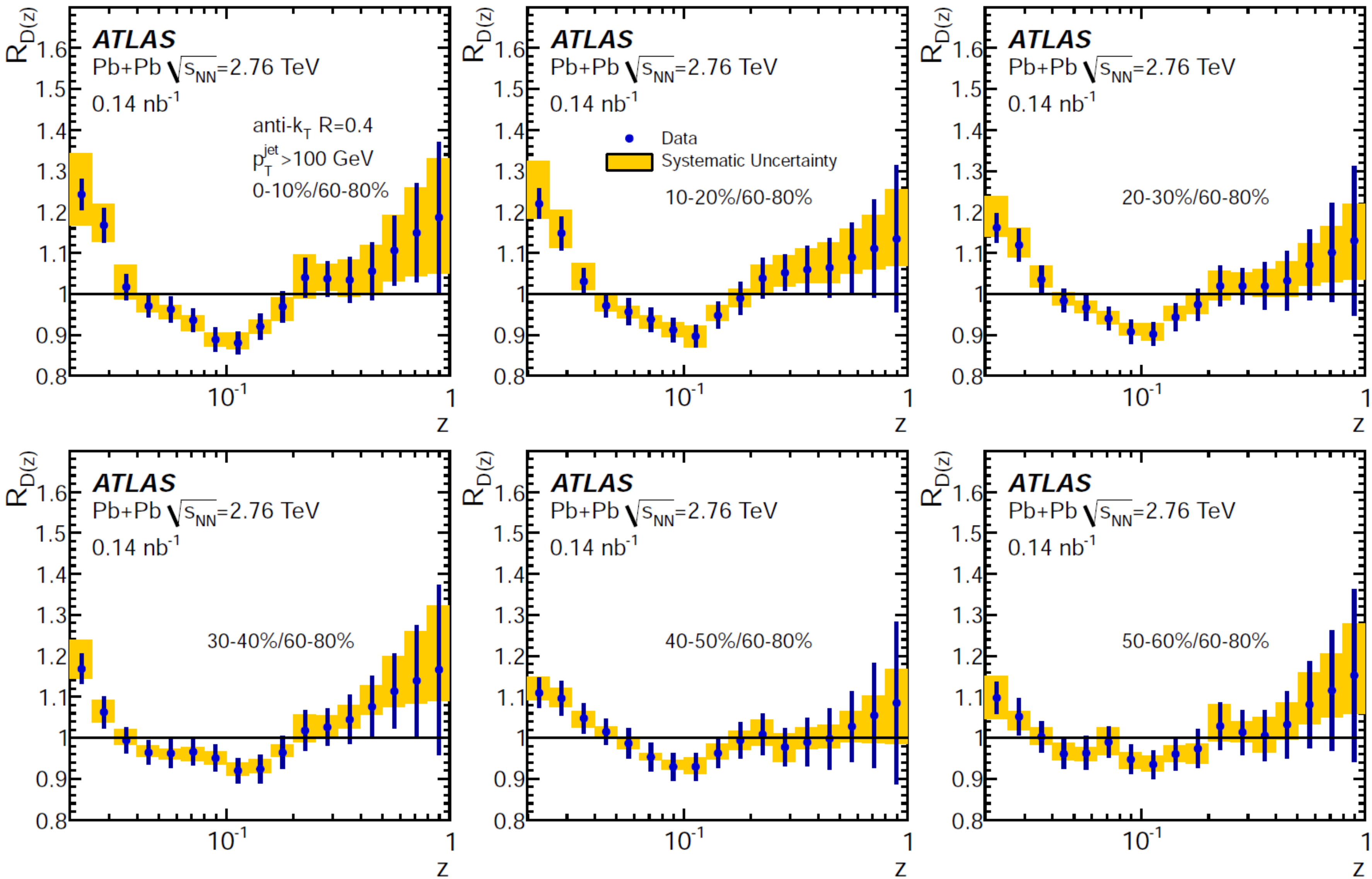

Full set of $R_{D(pt)}$ for R=0.4 jets

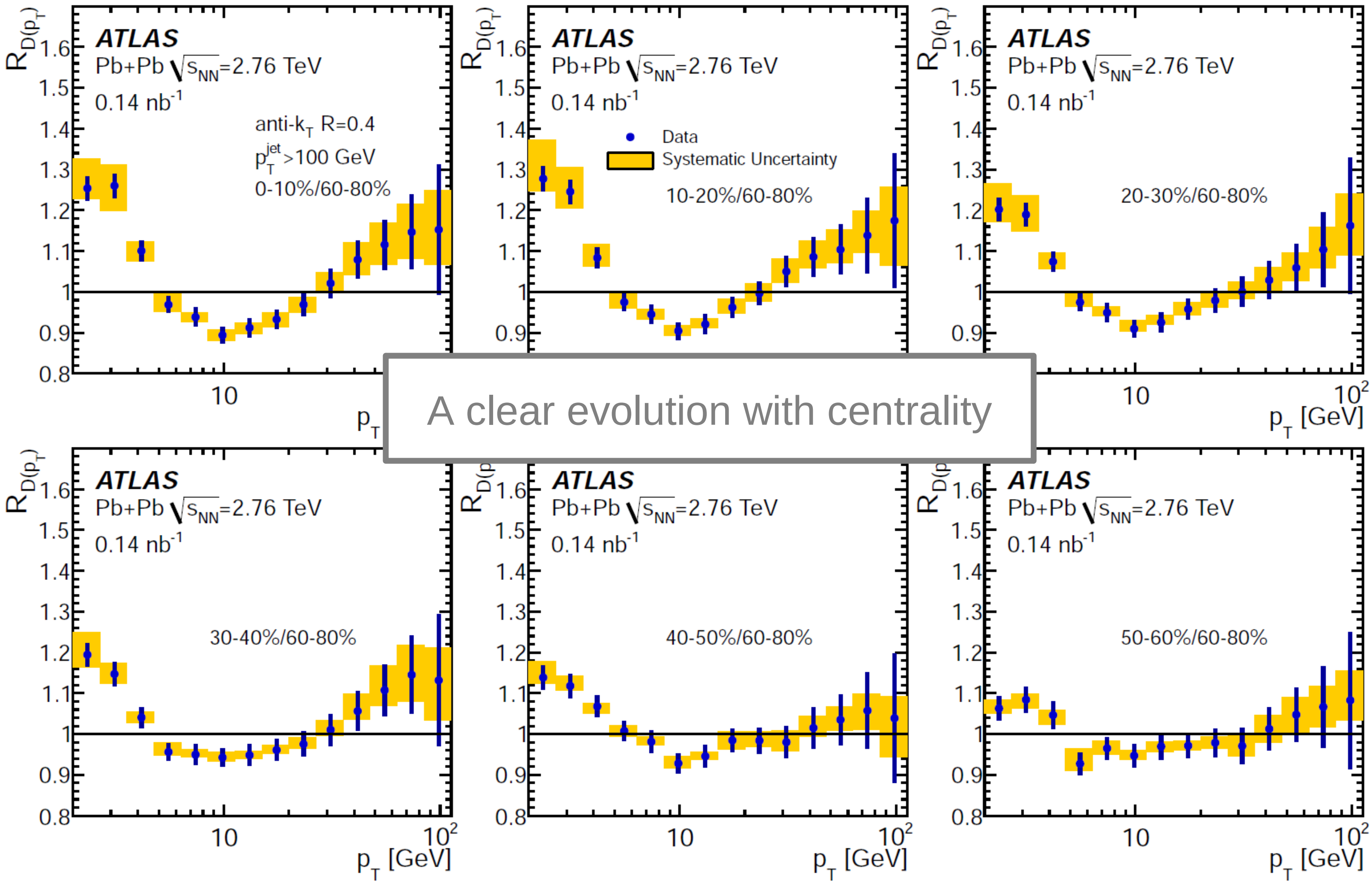

A clear evolution with centrality

Fragmentation for different jet radii

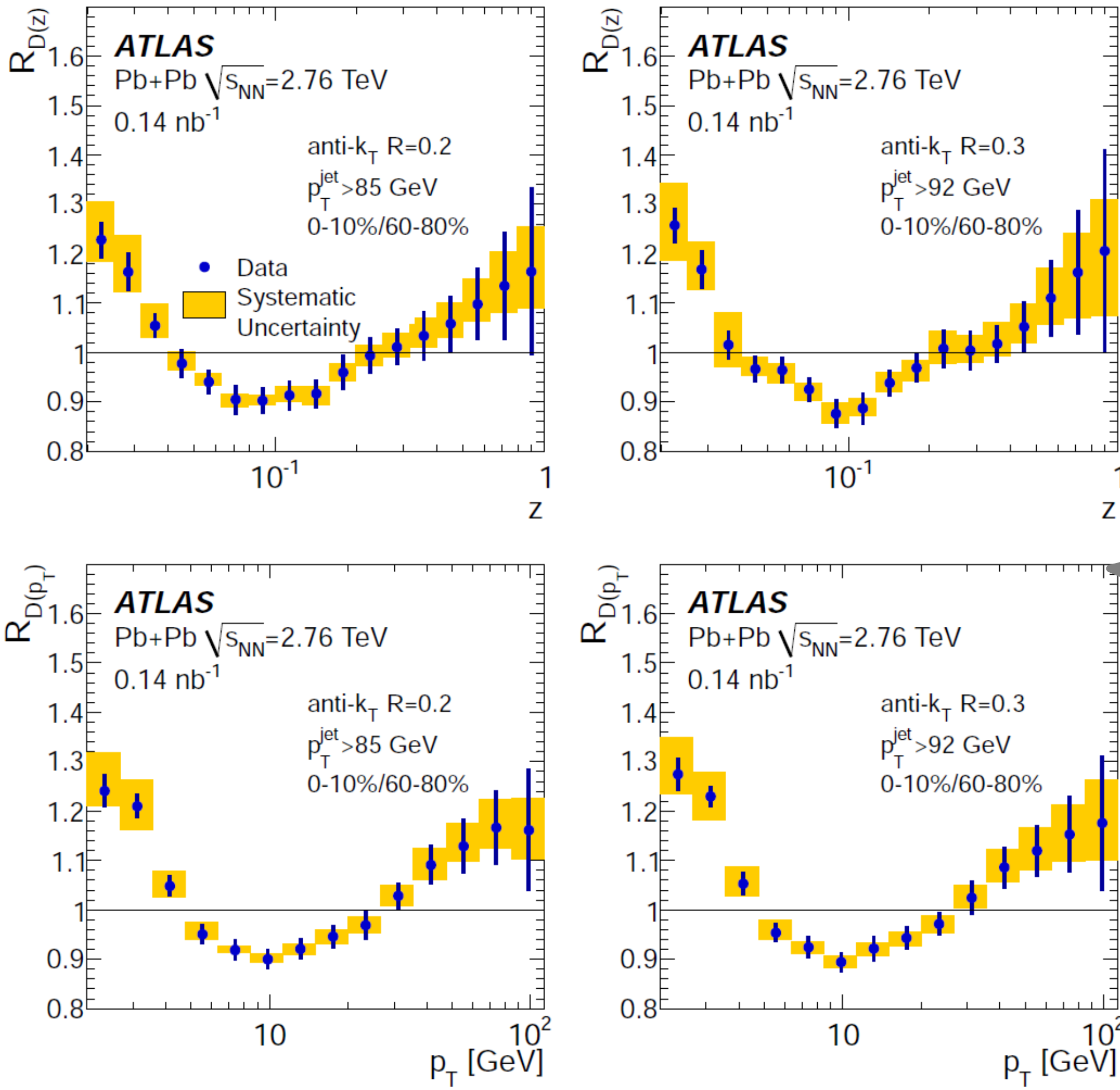

Results from R=0.4 jets are consistent with results from R=0.2 and R=0.3 jets

Quantifying the difference using $\Delta D(z)=D(z)|_{cent} - D(z)|_{60\text{-}80}$

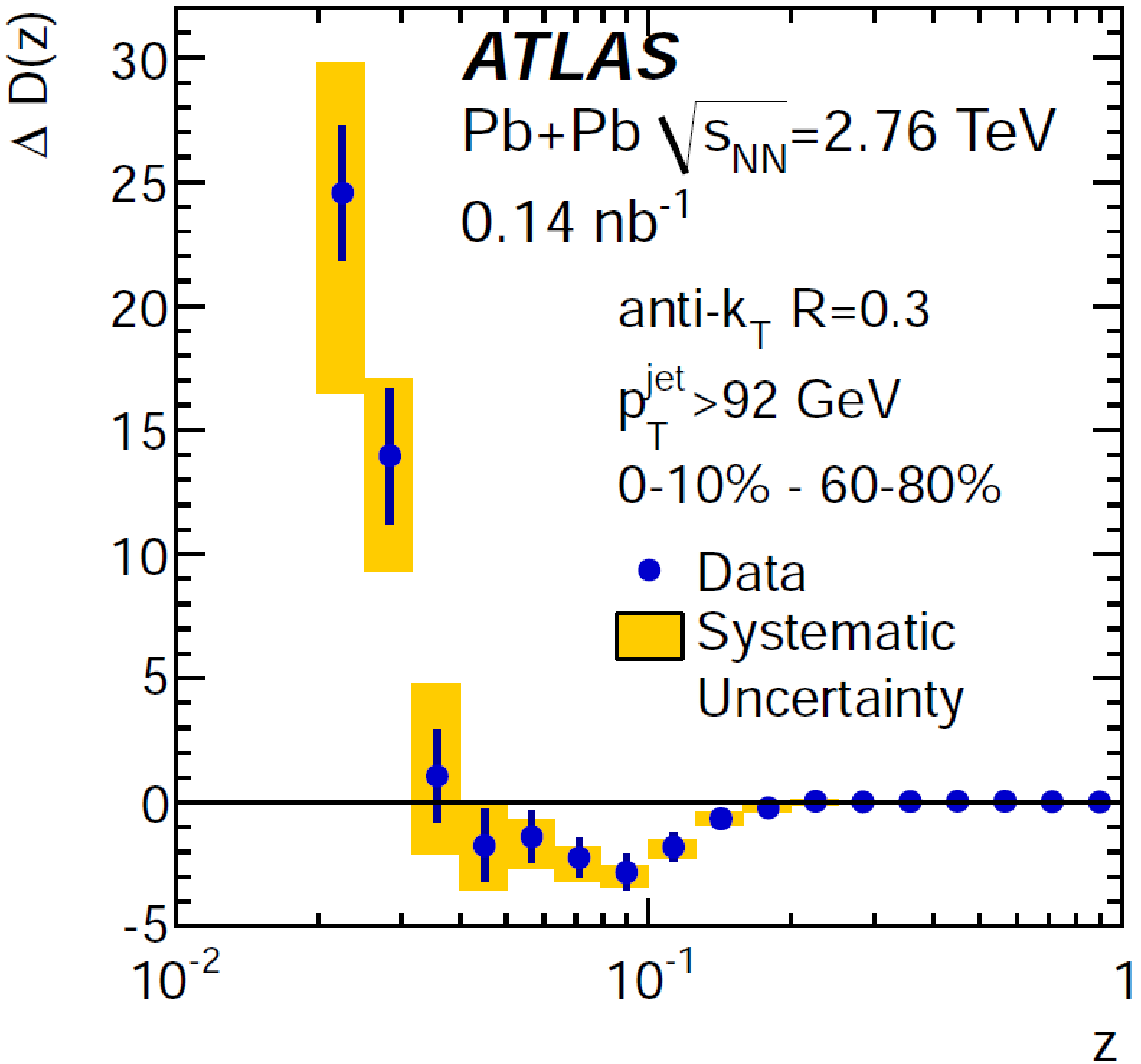

Quantifying the difference using $\Delta D(z)=D(z)|_{cent}-D(z)|_{60\text{-}80}$

Excess carried by less than one particle

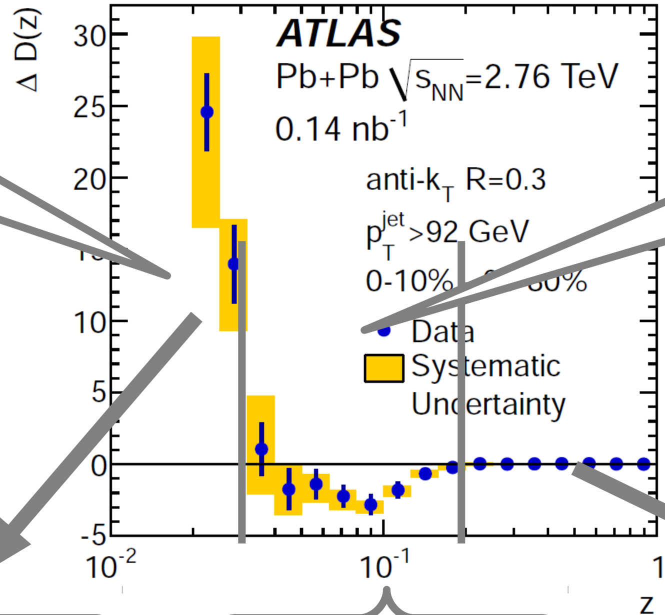

Suppression carried by ~one particle (14% of jet p_T)

No significant change in the number of high-p_T particles

centrality	$z = 0.02 - 0.04$		$z = 0.04 - 0.2$		$z = 0.4 - 1.0$	
	$\int \Delta D(z)dz$	$\int z\Delta D(z)dz$	$\int \Delta D(z)dz$	$\int z\Delta D(z)dz$	$\int \Delta D(z)dz$	$\int z\Delta D(z)dz$
0-10%	$0.65^{+0.21}_{-0.20}$	$0.017^{+0.006}_{-0.005}$	$-1.7^{+0.5}_{-0.6}$	$-0.14^{+0.04}_{-0.05}$	$0.07^{+0.05}_{-0.04}$	$0.037^{+0.030}_{-0.022}$
10-20%	$0.60^{+0.16}_{-0.16}$	$0.016^{+0.005}_{-0.004}$	$-1.6^{+0.7}_{-0.7}$	$-0.12^{+0.05}_{-0.05}$	$0.08^{+0.05}_{-0.04}$	$0.046^{+0.029}_{-0.025}$
20-30%	$0.48^{+0.11}_{-0.14}$	$0.013^{+0.003}_{-0.004}$	$-1.6^{+0.6}_{-0.5}$	$-0.13^{+0.04}_{-0.04}$	$0.04^{+0.05}_{-0.04}$	$0.026^{+0.029}_{-0.024}$
30-40%	$0.44^{+0.11}_{-0.15}$	$0.011^{+0.003}_{-0.004}$	$-1.4^{+0.6}_{-0.7}$	$-0.11^{+0.05}_{-0.05}$	$0.07^{+0.04}_{-0.05}$	$0.044^{+0.021}_{-0.028}$
40-50%	$0.33^{+0.09}_{-0.14}$	$0.009^{+0.003}_{-0.004}$	$-1.0^{+0.6}_{-0.8}$	$-0.09^{+0.04}_{-0.06}$	$-0.03^{+0.05}_{-0.04}$	$-0.011^{+0.030}_{-0.020}$
50-60%	$0.27^{+0.12}_{-0.18}$	$0.007^{+0.003}_{-0.005}$	$-1.0^{+0.8}_{-0.7}$	$-0.07^{+0.06}_{-0.06}$	$0.04^{+0.04}_{-0.05}$	$0.027^{+0.024}_{-0.029}$

Extending D(z) distributions

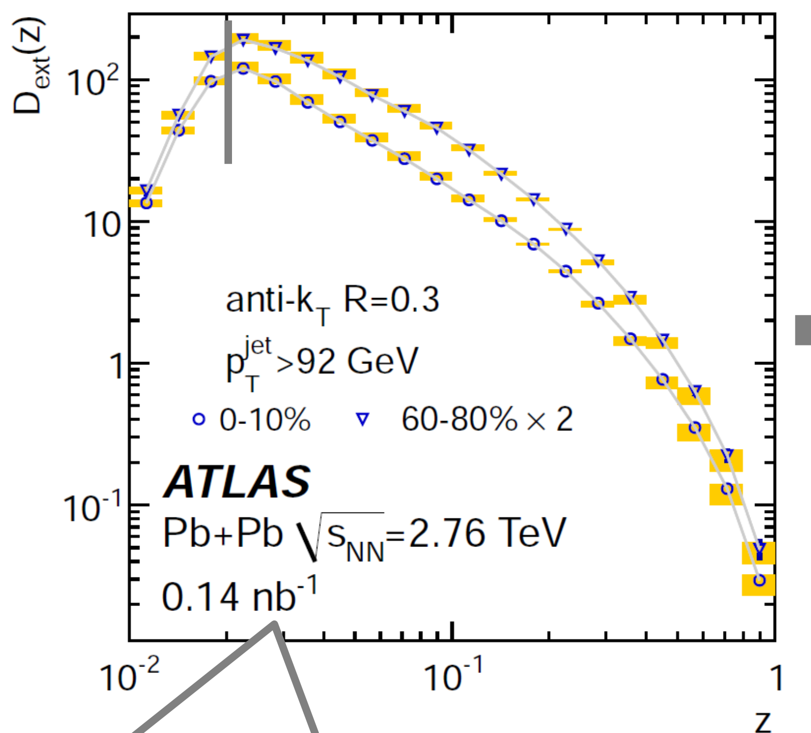

ratio

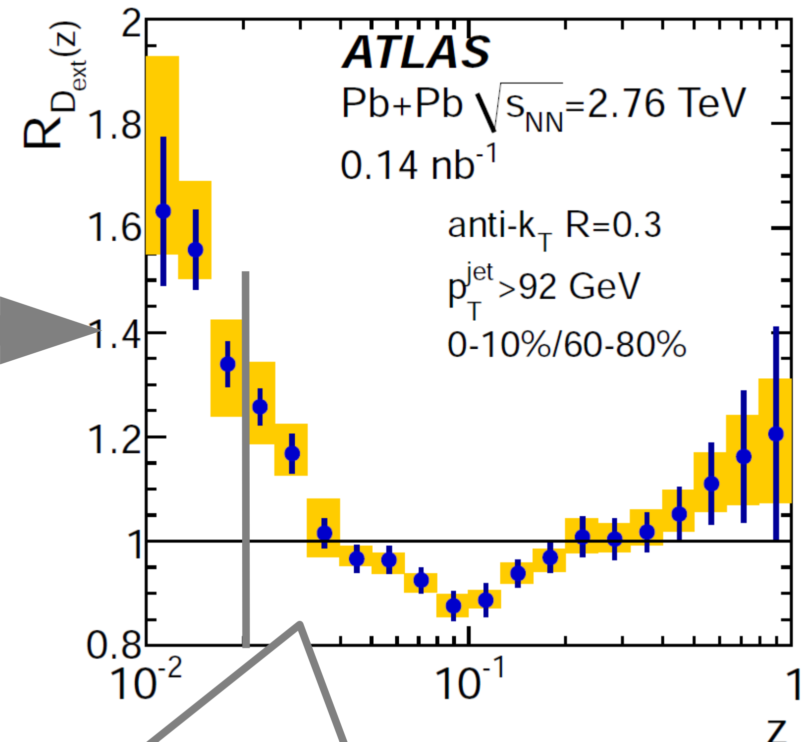

"Extended" D(z) distributions below z=0.02, that is a cut-off corresponding to track p_T of 2 GeV if reconstructed in a jet with p_T=100 GeV.

Corresponding ratio continues growing rapidly below z=0.02.

D(z) recalculated to D(ξ)

D(z) recalculated to D(ξ) that was previously measured by CMS.

Direct quantitative comparison with CMS not possible due to different kinematic cuts and acceptance

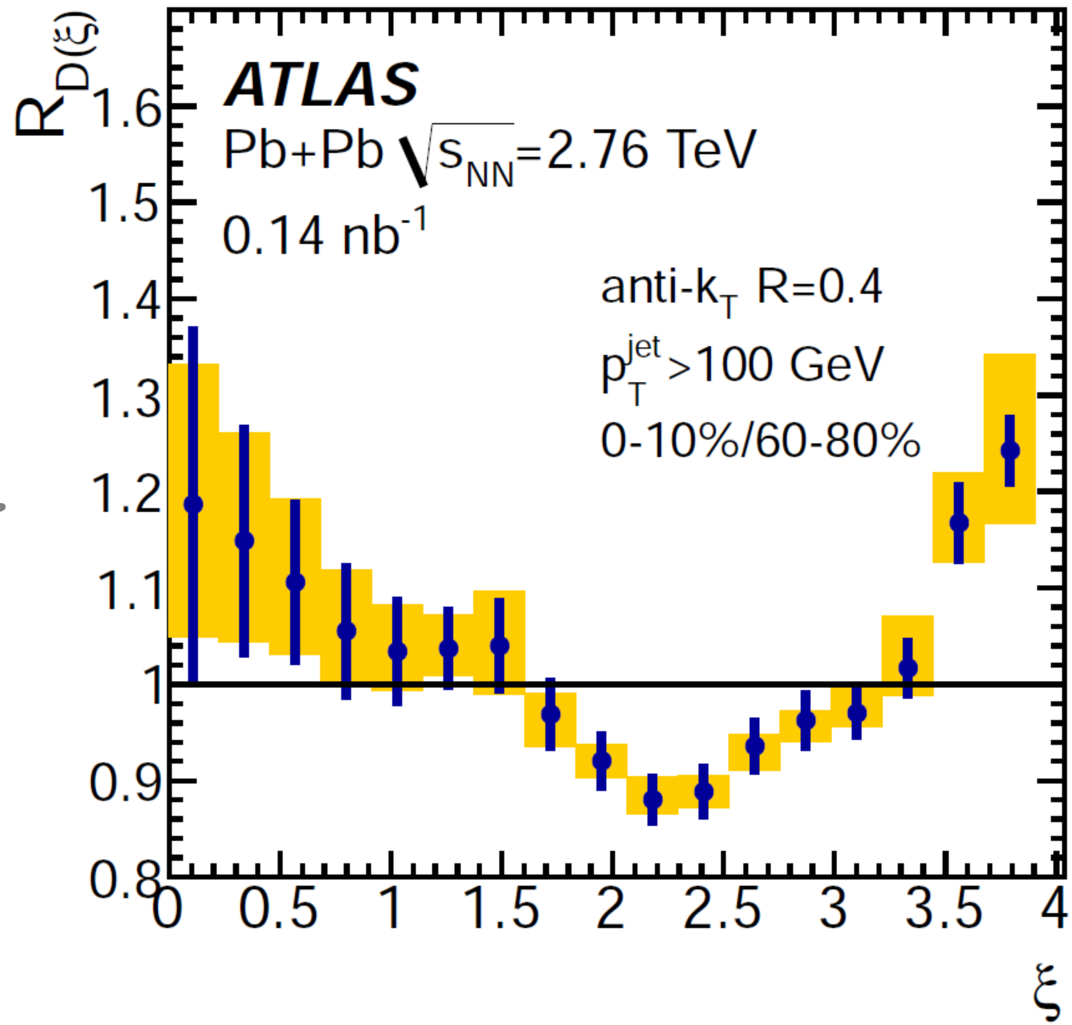

Neighboring jet production

Neighboring jet production

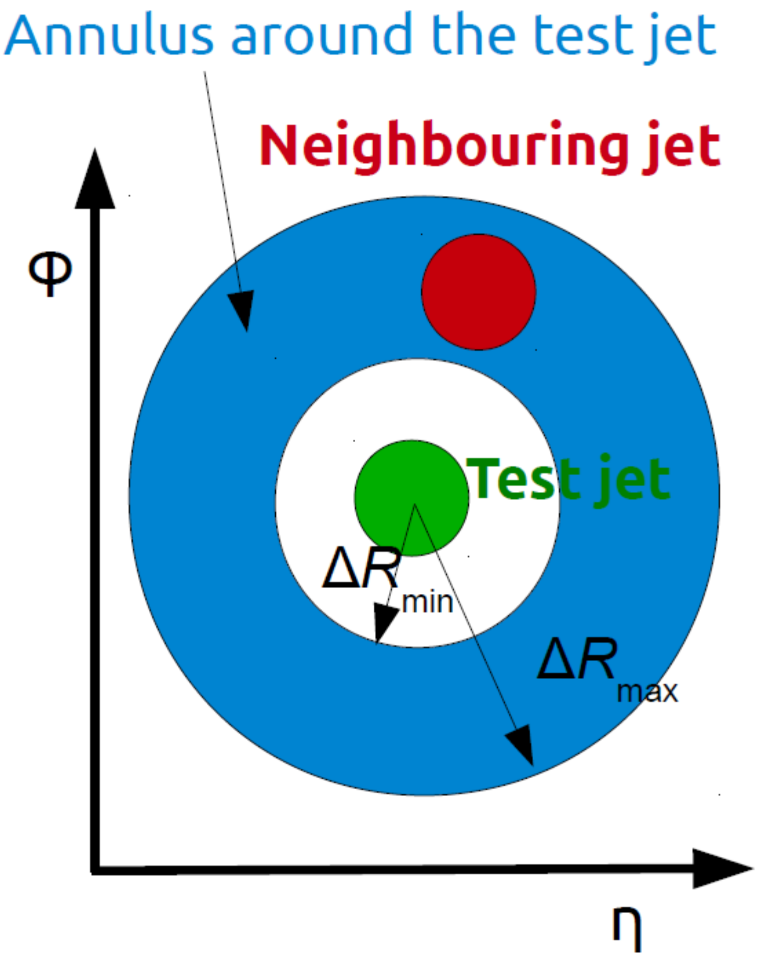

- May help understanding the differences in the quenching of the two jets that do not result from the difference in the path length.
- May help understanding the role of mini-jets / hard gluon radiation.
- May help constraining the modifications of the parton shower.

Neighboring jet production

- Neighboring jet production quantified using quantity previously measured at Tevatron

$$R_{\Delta R} = \frac{1}{\mathrm{d}N_{\mathrm{jet}}^{\mathrm{test}}/\mathrm{d}E_{\mathrm{T}}^{\mathrm{test}}} \sum_{i=1}^{N_{\mathrm{jet}}^{\mathrm{test}}} \frac{\mathrm{d}N_{\mathrm{jet},i}^{\mathrm{nbr}}}{\mathrm{d}E_{\mathrm{T}}^{\mathrm{test}}}(E_{\mathrm{T}}^{\mathrm{test}}, E_{\mathrm{T,min}}^{\mathrm{nbr}}, \Delta R)$$

… the rate of neighboring jets that accompany a given test jet.

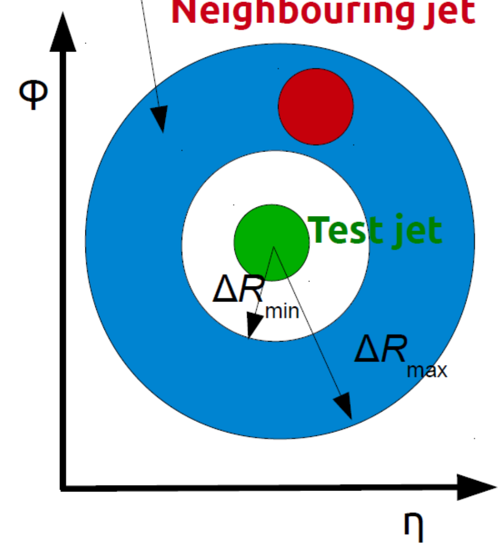

- $R_{\Delta R}$ evaluated also differentially in neighboring jet Et

$$\frac{\mathrm{d}R_{\Delta R}}{\mathrm{d}E_{\mathrm{T}}^{\mathrm{nbr}}} = \frac{1}{\mathrm{d}N_{\mathrm{jet}}^{\mathrm{test}}/\mathrm{d}E_{\mathrm{T}}^{\mathrm{test}}} \sum_{i=1}^{N_{\mathrm{jet}}^{\mathrm{test}}} \frac{\mathrm{d}^2 N_{\mathrm{jet},i}^{\mathrm{nbr}}}{\mathrm{d}E_{\mathrm{T}}^{\mathrm{test}}\mathrm{d}E_{\mathrm{T}}^{\mathrm{nbr}}}(E_{\mathrm{T,min}}^{\mathrm{test}}, E_{\mathrm{T}}^{\mathrm{nbr}}, \Delta R)$$

… which are the E_T spectra of the third (or n^{th}) jet given the test jet E_T

- To quantify the centrality dependence the central-to-peripheral ratios, $\rho(R_{\Delta R})$, also evaluated

Binning of the measurement

- 3 jet sizes: d=0.2, 0.3, and 0.4 jets (change in the notation for this analysis "d" is the jet size parameter "R")
- 5 bins in the test jet E_T
- 4 bins in the neighboring jet E_T
- Four centrality bins: 0 - 10% - 20% - 40% - 80%
- The size of the annulus: $\Delta R_{min} < \Delta R < 1.6$, where
  - ΔR_{min} = 0.8 (d=0.4 jet)
  - ΔR_{min} = 0.6 (d=0.3 jets)
  - ΔR_{min} = 0.5 (d=0.2 jets)
- Measurement restricted over the range with well understood detector response, $|\eta|<2.8$ => test jet cut of $|\eta|<1.2$

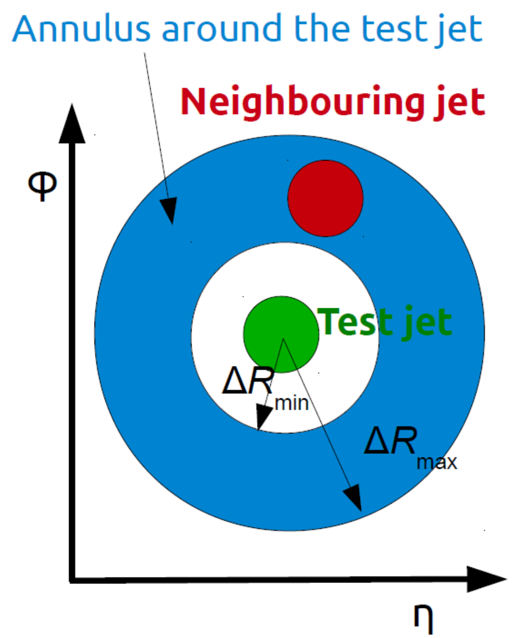

Important experimental corrections

- Fake jets rejected using standard procedure of matching to clusters and track jets.
- Jet E_T corrected to reduce the effect of up-feeding due to finite JER.
- Contribution from two independent hard processes subtracted using the estimate of the rate from the MC to data overlay.

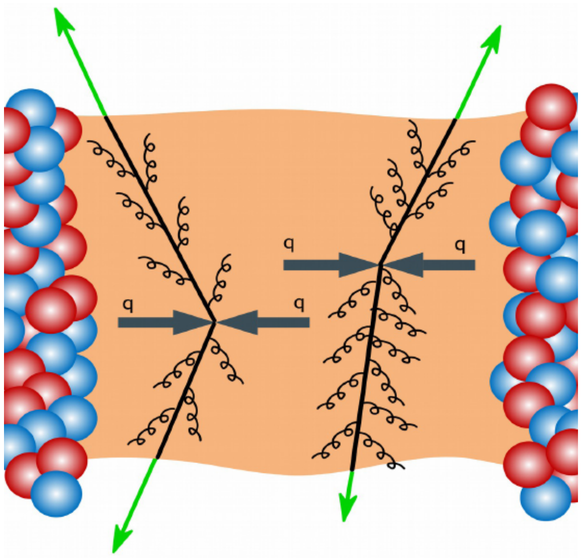

- Distributions need to be further corrected, e.g. for the case when two neighboring jets overlap
- Bin-by-bin correction applied to correct for:
  - effects due to finite jet energy resolution and jet reconstruction efficiency
  - migration in/out of the jet annulus due to finite jet position resolution

Efficiency and bin-by-bin corrections

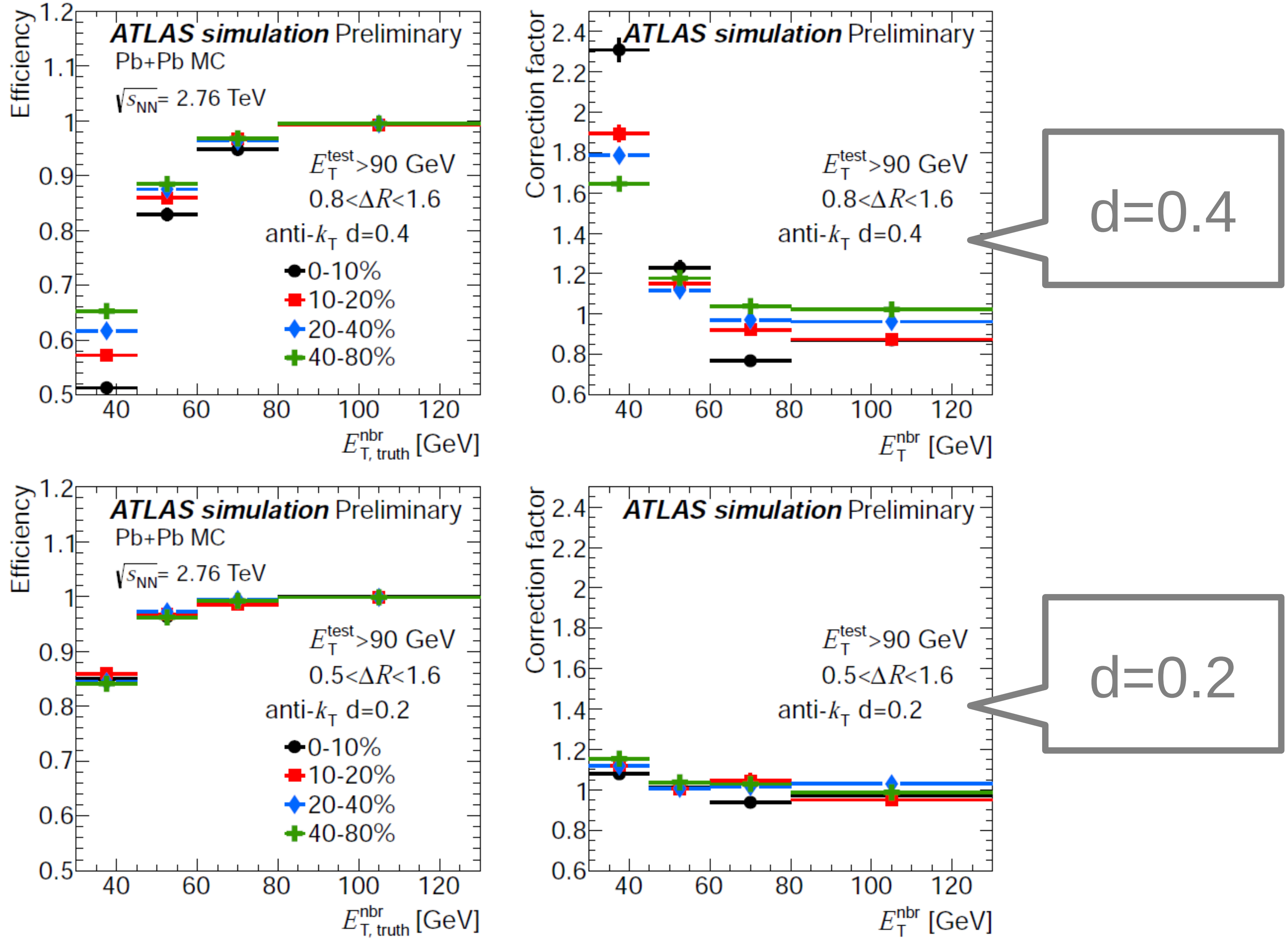

Correction flow

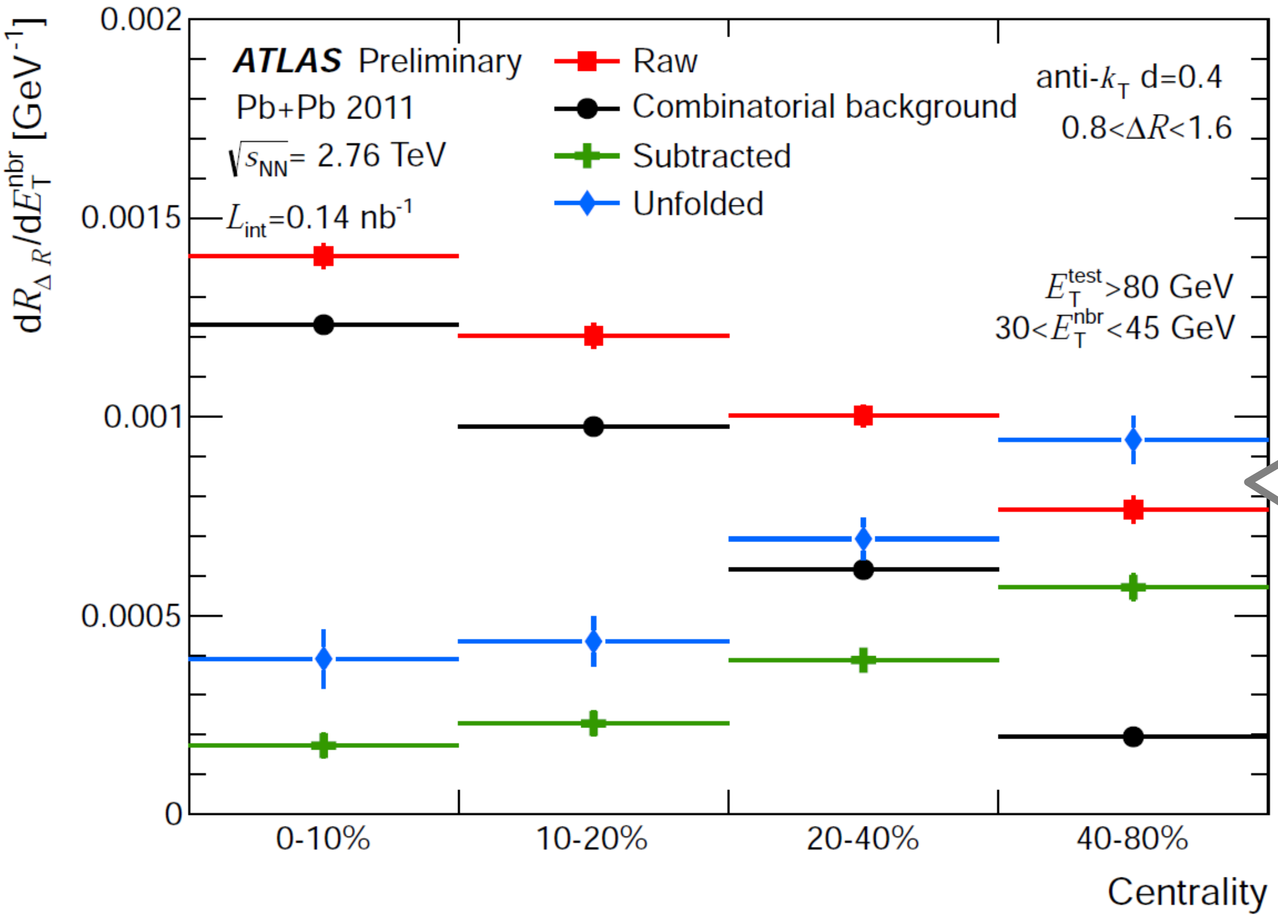

Example of the correction flow for the most “difficult” case of lowest E_T bins

Unfolded = *k* * (Raw – Combinatorics)

$R_{\Delta R}$ – test jet Et dependence

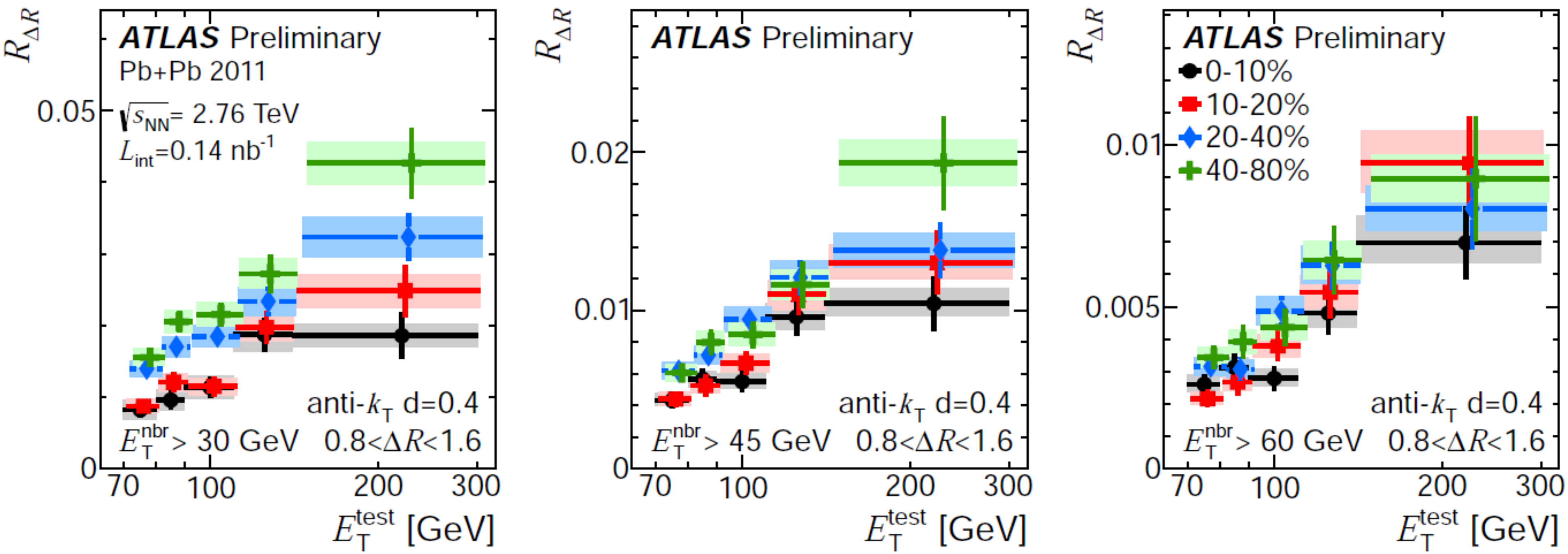

- Monotonic increase with increasing test jet E_T (shape already known from $p\bar{p}$ D0).
- Clear trends of suppression with increasing centrality.

$R_{\Delta R}$ – neighboring jet E_T dependence

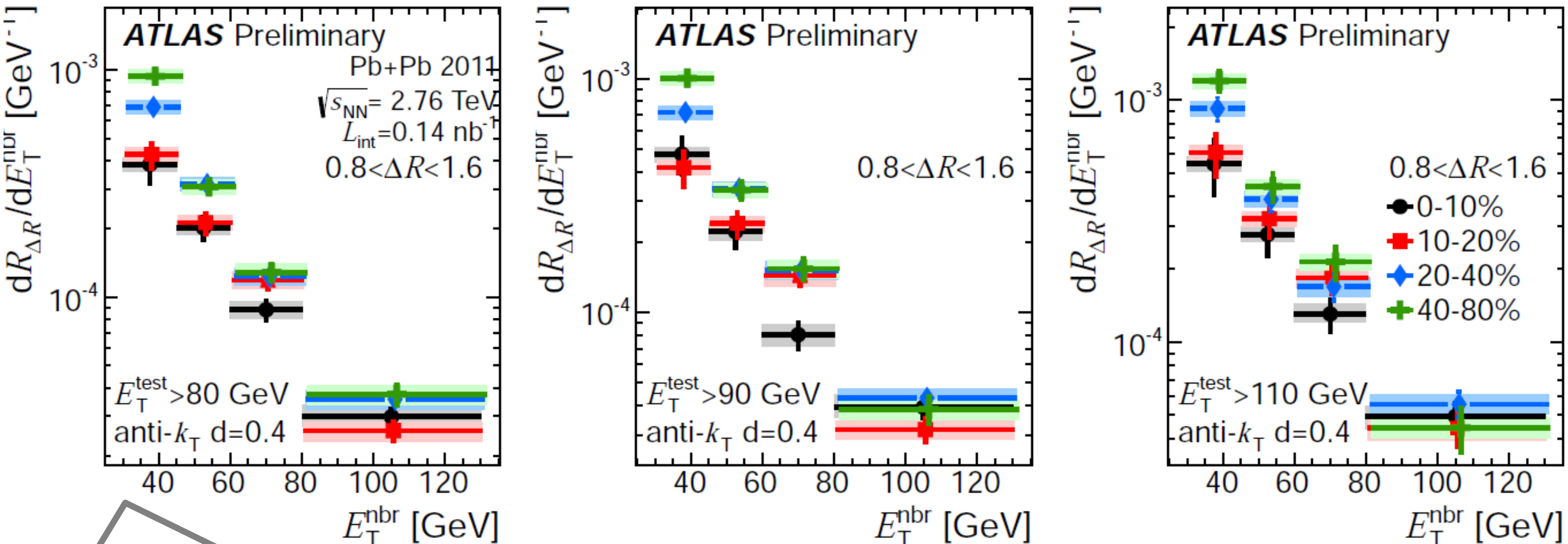

Same trends of the suppression but less clear to see in the falling spectra

	0–10%	10–20%	20–40%	40–80%
$d = 0.4$	2.66 ± 0.23	2.72 ± 0.22	2.93 ± 0.15	3.29 ± 0.21
$d = 0.3$	2.75 ± 0.21	2.45 ± 0.20	2.95 ± 0.16	3.23 ± 0.19
$d = 0.2$	2.76 ± 0.19	2.58 ± 0.19	2.67 ± 0.17	3.00 ± 0.20

Spectral index from a power law fit. Centrality dependence of the spectral index: more central = less steep.

Central-to-peripheral ratios

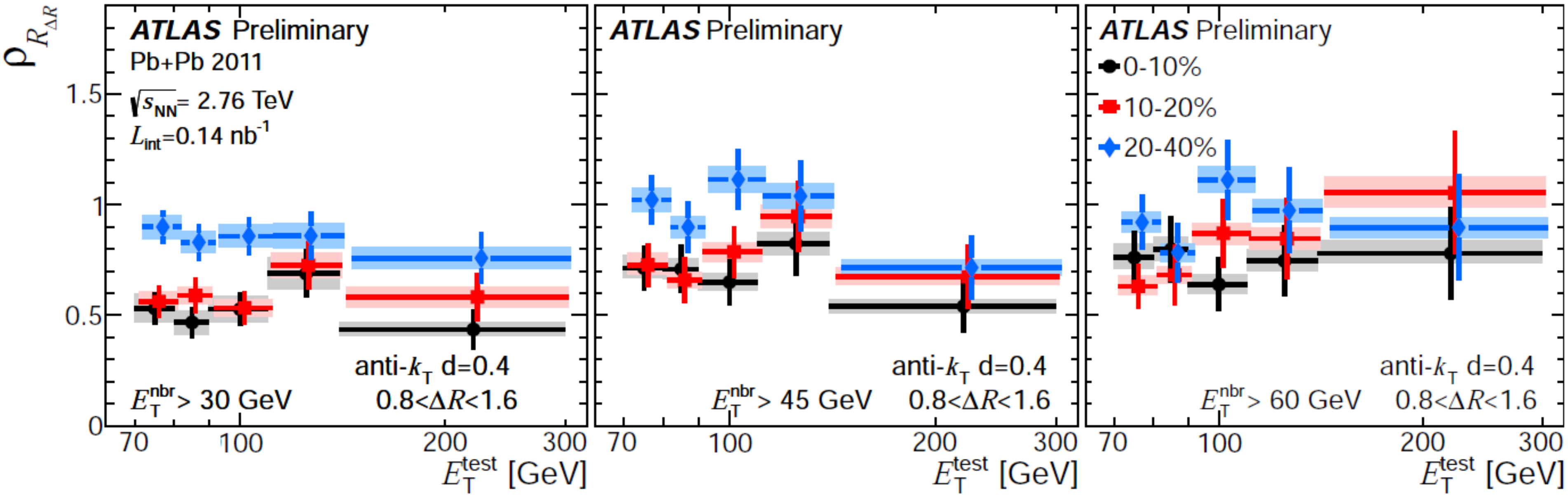

Central to peripheral ratio of $R_{\Delta R}$ as a function of <u>test jet E_T</u>.

–> suppression factor of about 0.5

–> suppression rather flat with E_T

} similar trends as in the inclusive jet R_{CP}

Central-to-peripheral ratios

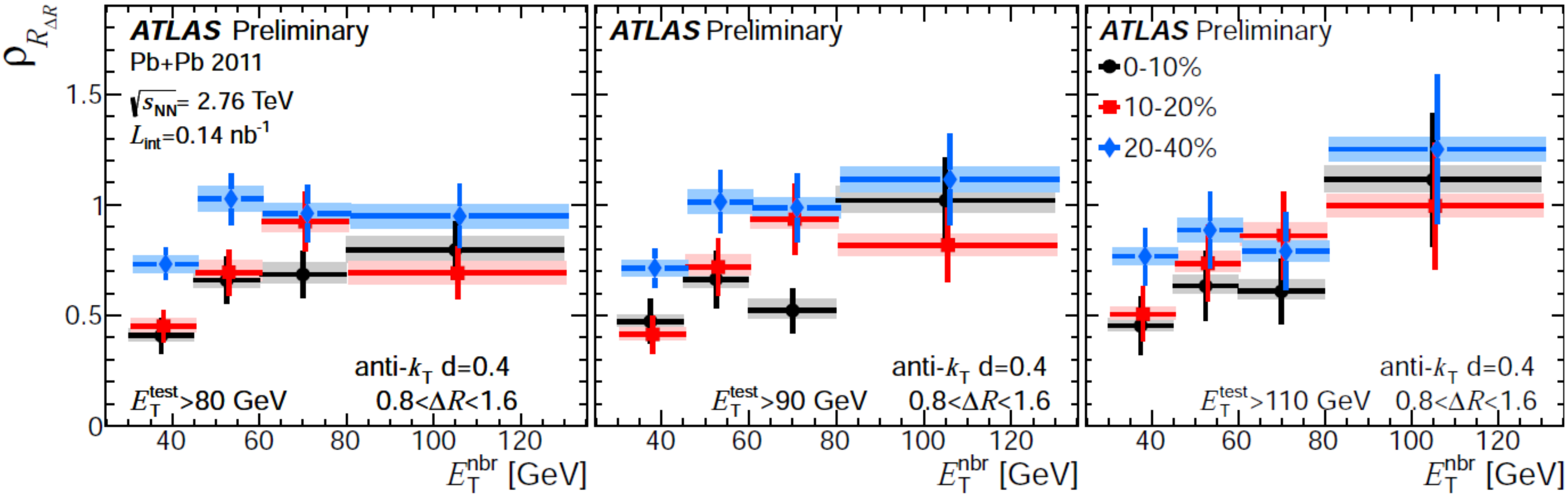

Central to peripheral ratio of $R_{\Delta R}$ as a function of neighboring jet E_T.
Decrease of suppression with increasing jet E_T … may be expected for the configuration of magnitude of neighboring jet E_T approaching the magnitude of test jet E_T (the per-test jet normalization in the $R_{\Delta R}$ effectively removes the suppression).

Summary

- Jet fragmentation evaluated in terms of D(z) and D(p_T) distributions and their central-to-peripheral ratio for three different jet radii, six different centrality bins.
- A modest but significant modification of fragmentation seen: an enhancement in fragment yield in central collisions for $z < 0.04$, a reduction in fragment yield for $0.04 < z < 0.25$ and an enhancement in the fragment yield for $z > 0.25$.
- Neighboring jet rates, $R_{\Delta R}$, evaluated as a function of test jet E_T and neighboring jet E_T for three different jet radii and four centrality bins.
- Significant suppression seen in central collisions for the configuration when neighboring jet E_T is different from test jet E_T which has similar trends as the suppression in inclusive jets.
- Indication of the centrality dependence of the power-law index of neighboring E_T spectra.

Backup slides

Jet RAA

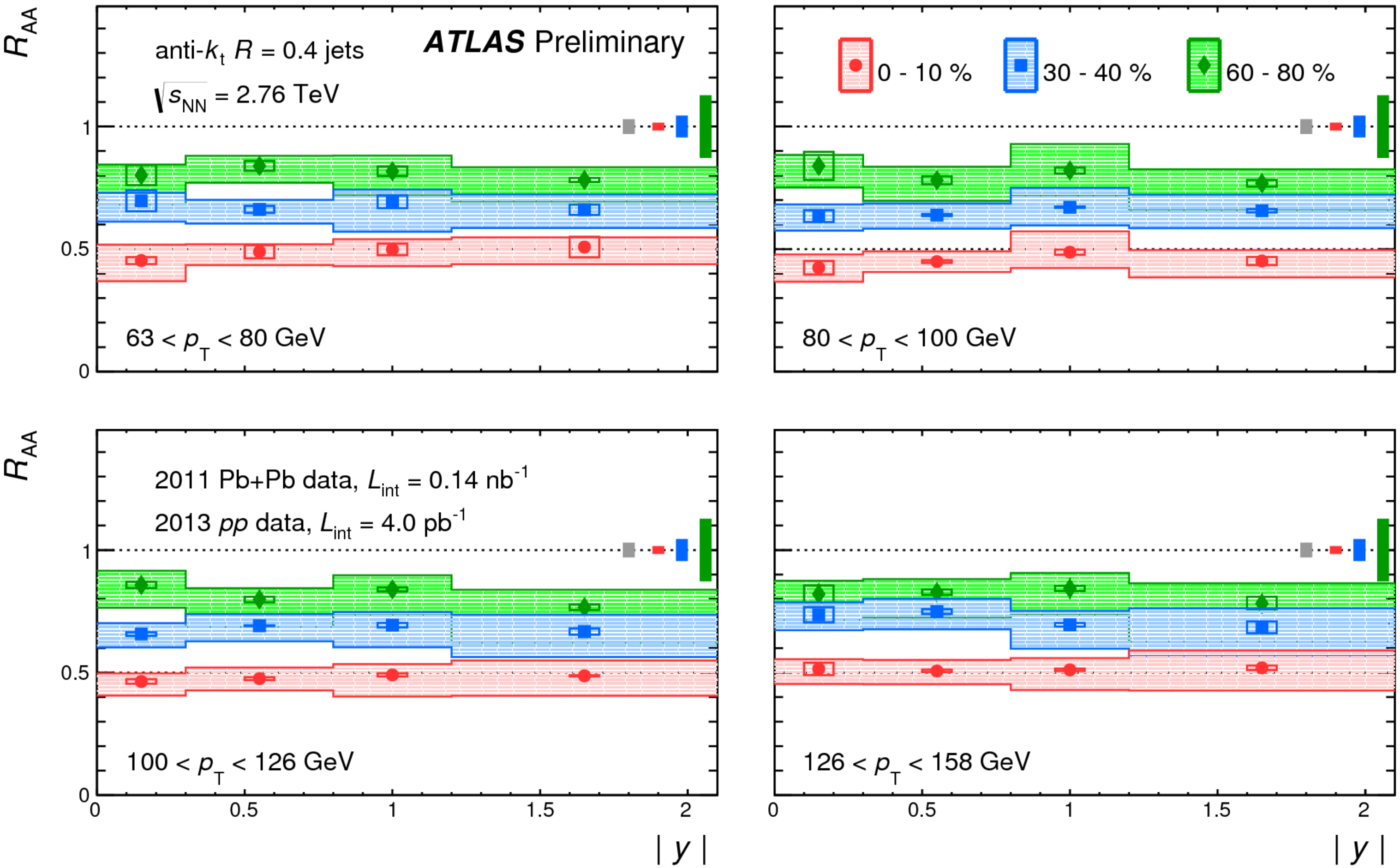

R_{AA}
anti-k_t R = 0.4 jets
ATLAS Preliminary
$\sqrt{s_{NN}}$ = 2.76 TeV
0 - 10 %
30 - 40 %
60 - 80 %
63 < p_T < 80 GeV
80 < p_T < 100 GeV
2011 Pb+Pb data, L_{int} = 0.14 nb^{-1}
2013 pp data, L_{int} = 4.0 pb^{-1}
100 < p_T < 126 GeV
126 < p_T < 158 GeV
| y |

Jet RAA

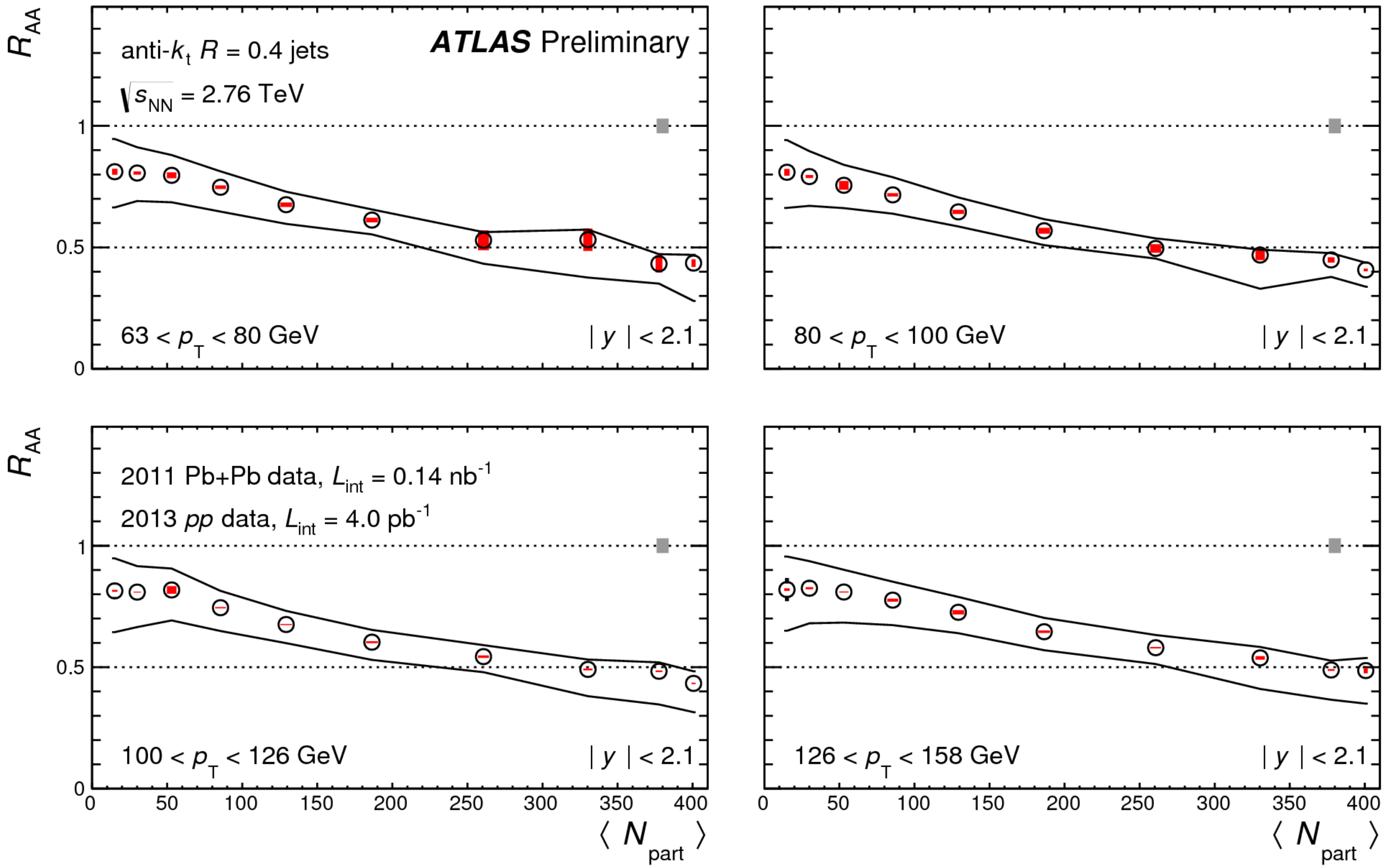

R_{AA}
anti-k_t R = 0.4 jets
ATLAS Preliminary
$\sqrt{s_{NN}}$ = 2.76 TeV
63 < p_T < 80 GeV
| y | < 2.1
80 < p_T < 100 GeV
| y | < 2.1
2011 Pb+Pb data, L_{int} = 0.14 nb^{-1}
2013 pp data, L_{int} = 4.0 pb^{-1}
100 < p_T < 126 GeV
| y | < 2.1
126 < p_T < 158 GeV
| y | < 2.1
⟨ N_{part} ⟩
0 50 100 150 200 250 300 350 400
0 0.5 1

Improvements in jet reconstruction over the first analyses

- The use of MC to real data overlay
- Improvements in the UE subtraction
- Improvements in the determination of the JES uncertainty:
  - Studying the response as a function of parton flavor and parton showers from different MC generators
  - Determine the response and uncertainty based on in-situ studies of gamma-jet and Z-jet correlations using in full 8 TeV pp data
  - Use the fragmentation measurement to judge the impact of modified fragmentation on JES uncertainty

Unfolding

- Correction from the reconstructed level to the truth level.
- Corrects mainly for jet energy and track momentum resolution.
- Singular value decomposition technique implemented in RooUnfold package used.

Example of the performance of unfolding for D(z) distributions

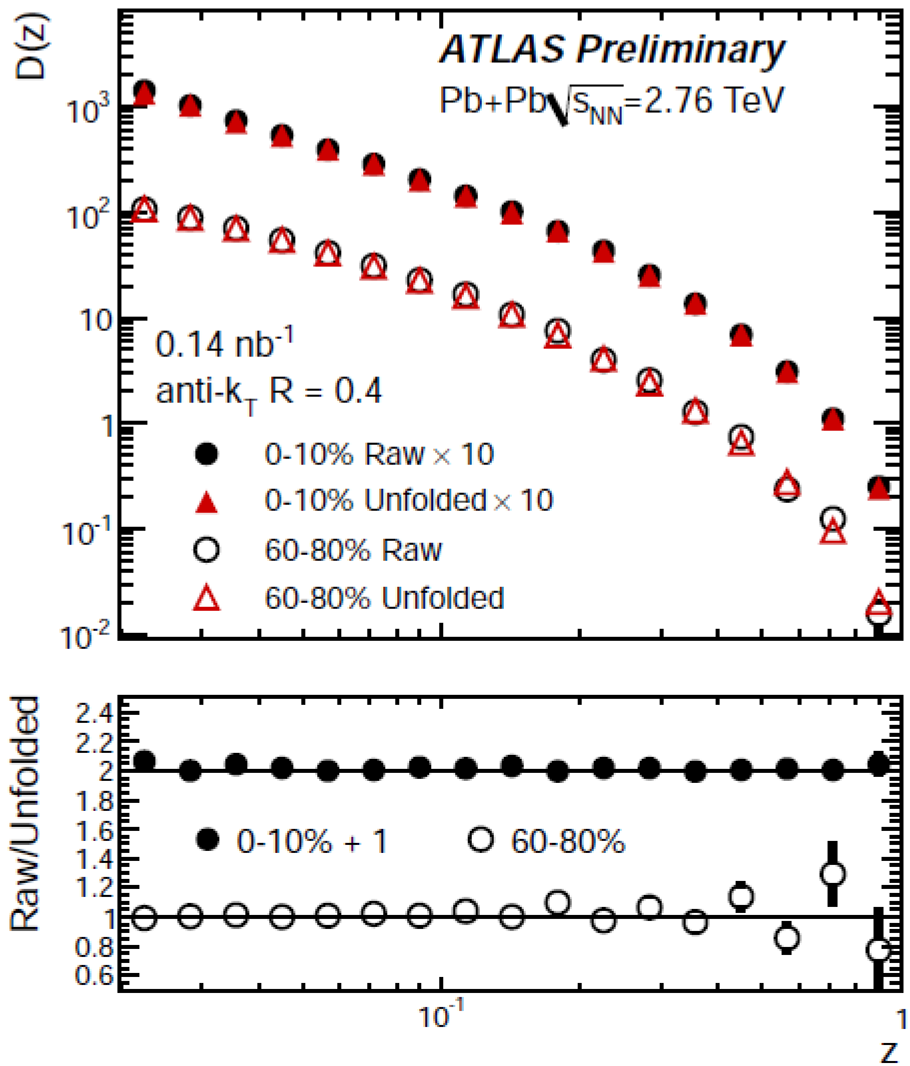

Unfolding performance for D(z)

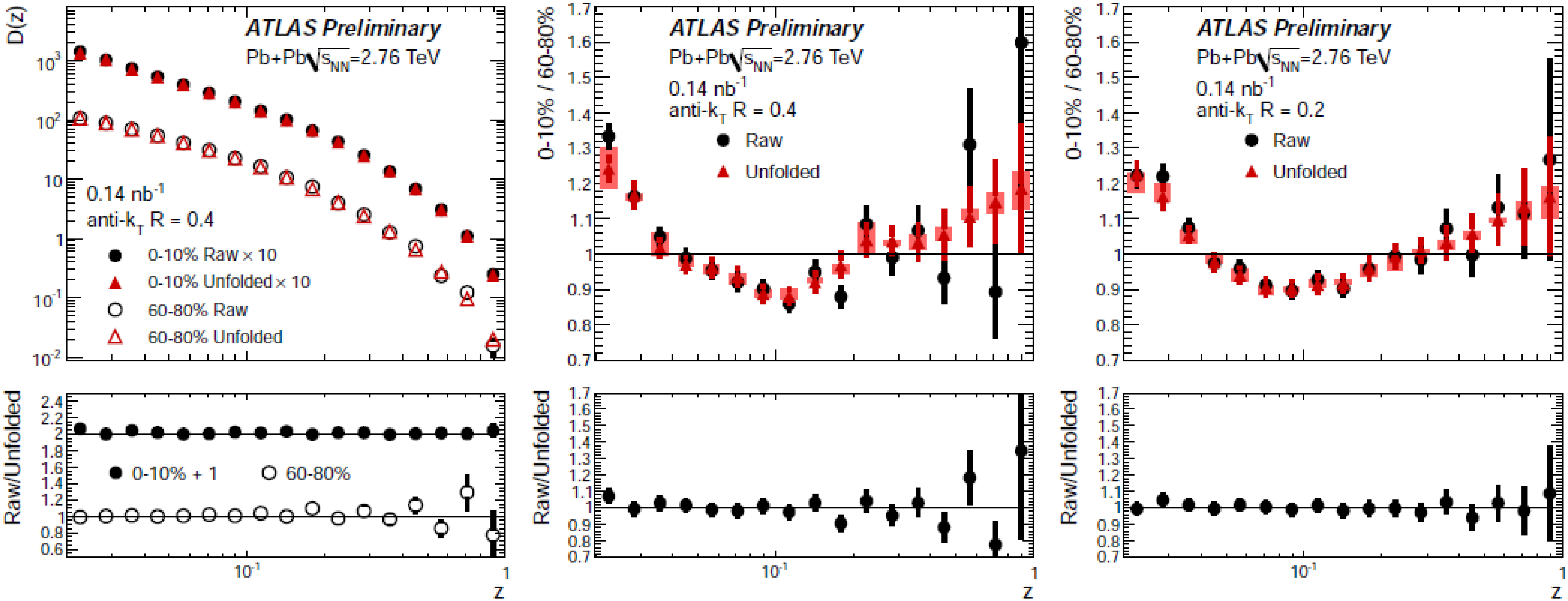

Unfolding

- Correction from the reconstructed level to the truth level.
- Corrects mainly for jet energy and track momentum resolution.
- Singular value decomposition technique implemented in RooUnfold package used.

Example of the performance of unfolding for $R_{D(z)}$ distributions

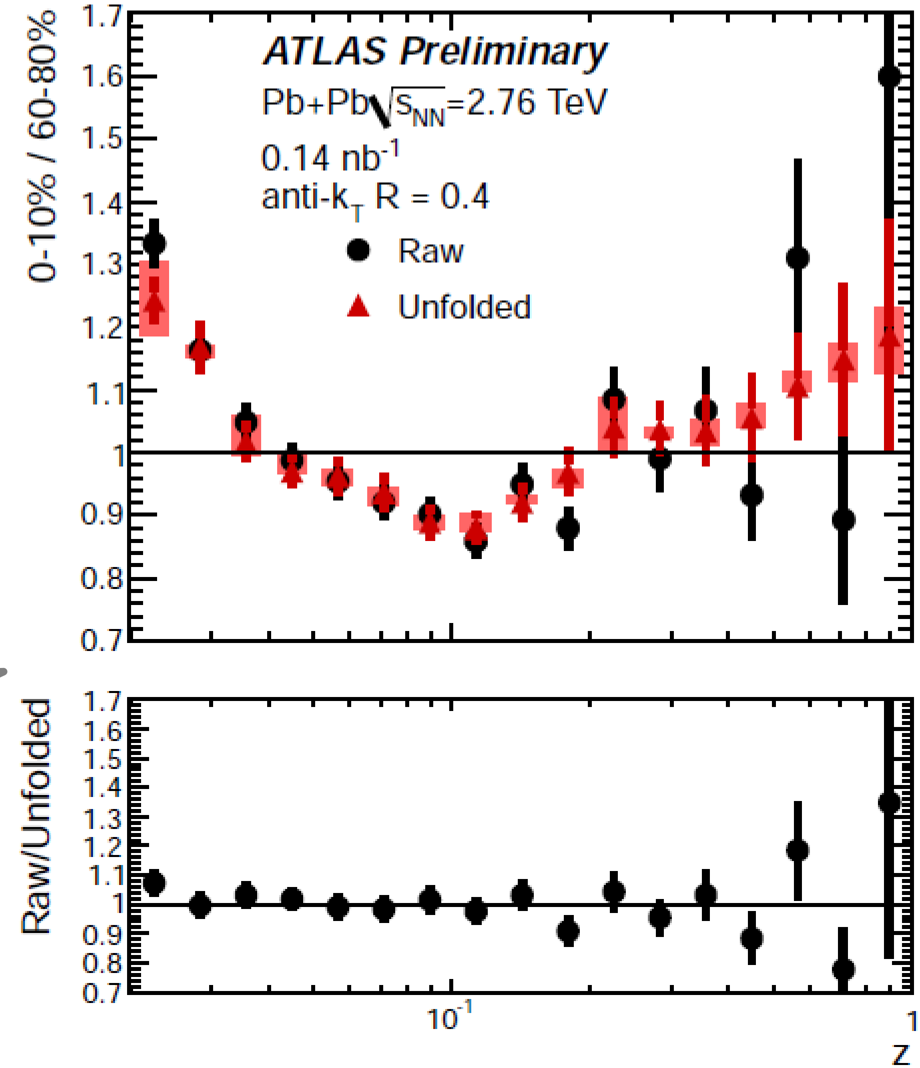

Unfolding performance for D(pt)

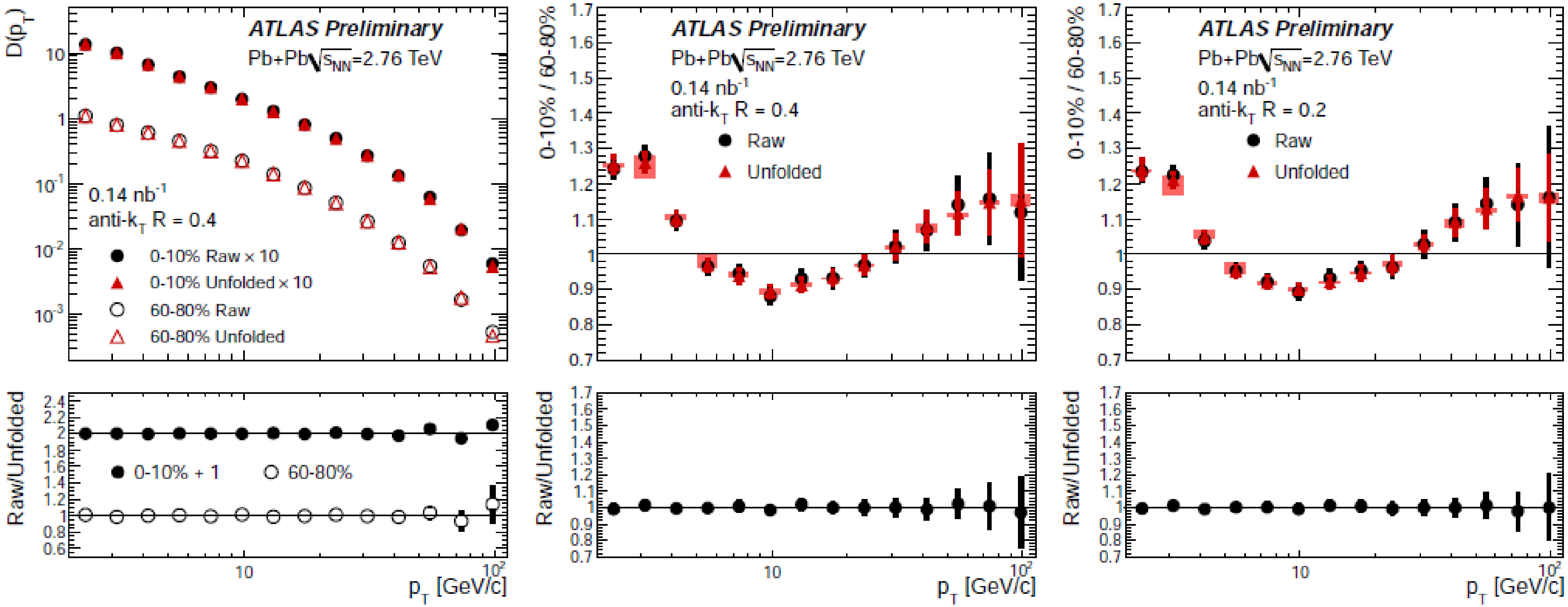

Ratios of D(ξ)

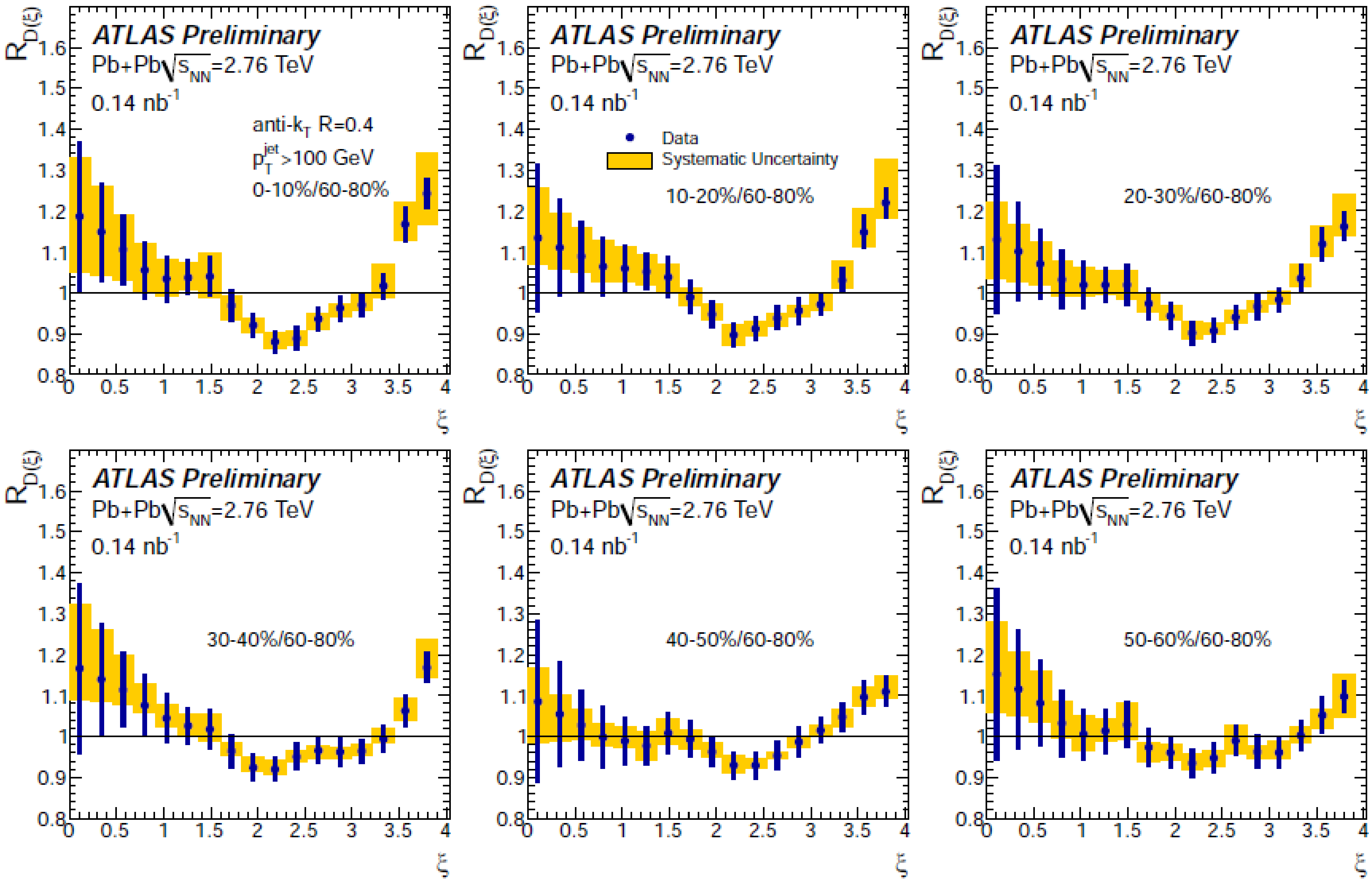

ATLAS Preliminary
Pb+Pb $\sqrt{s_{NN}}$=2.76 TeV
0.14 nb^{-1}
anti-k_T R=0.4
p_T^{jet}>100 GeV
0-10%/60-80%
Data
Systematic Uncertainty
10-20%/60-80%
20-30%/60-80%
30-40%/60-80%
40-50%/60-80%
50-60%/60-80%
$R_{D(\xi)}$
ξ

D(z) and D(pt) for R=0.2

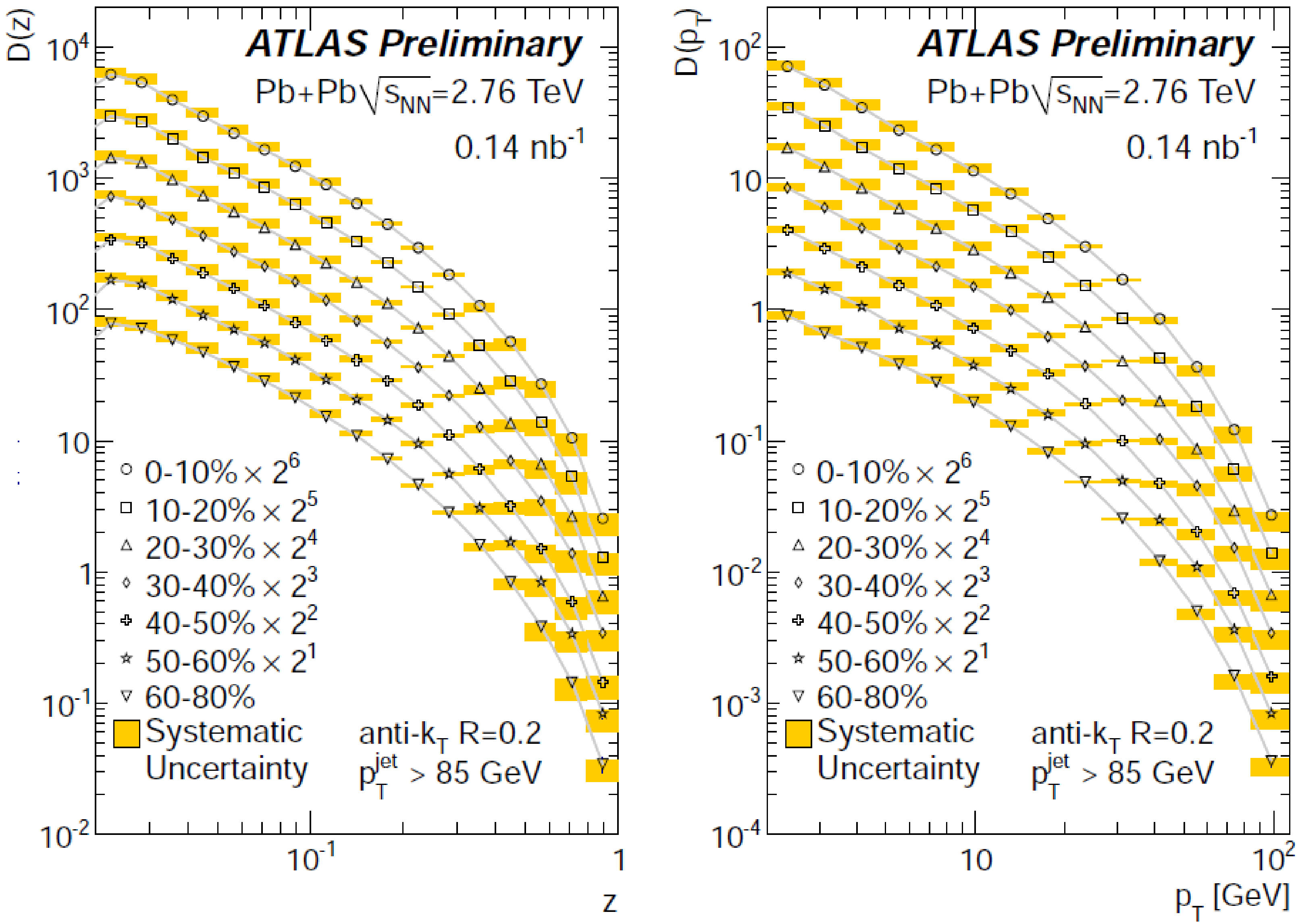

$R_{D(z)}$ for R=0.3

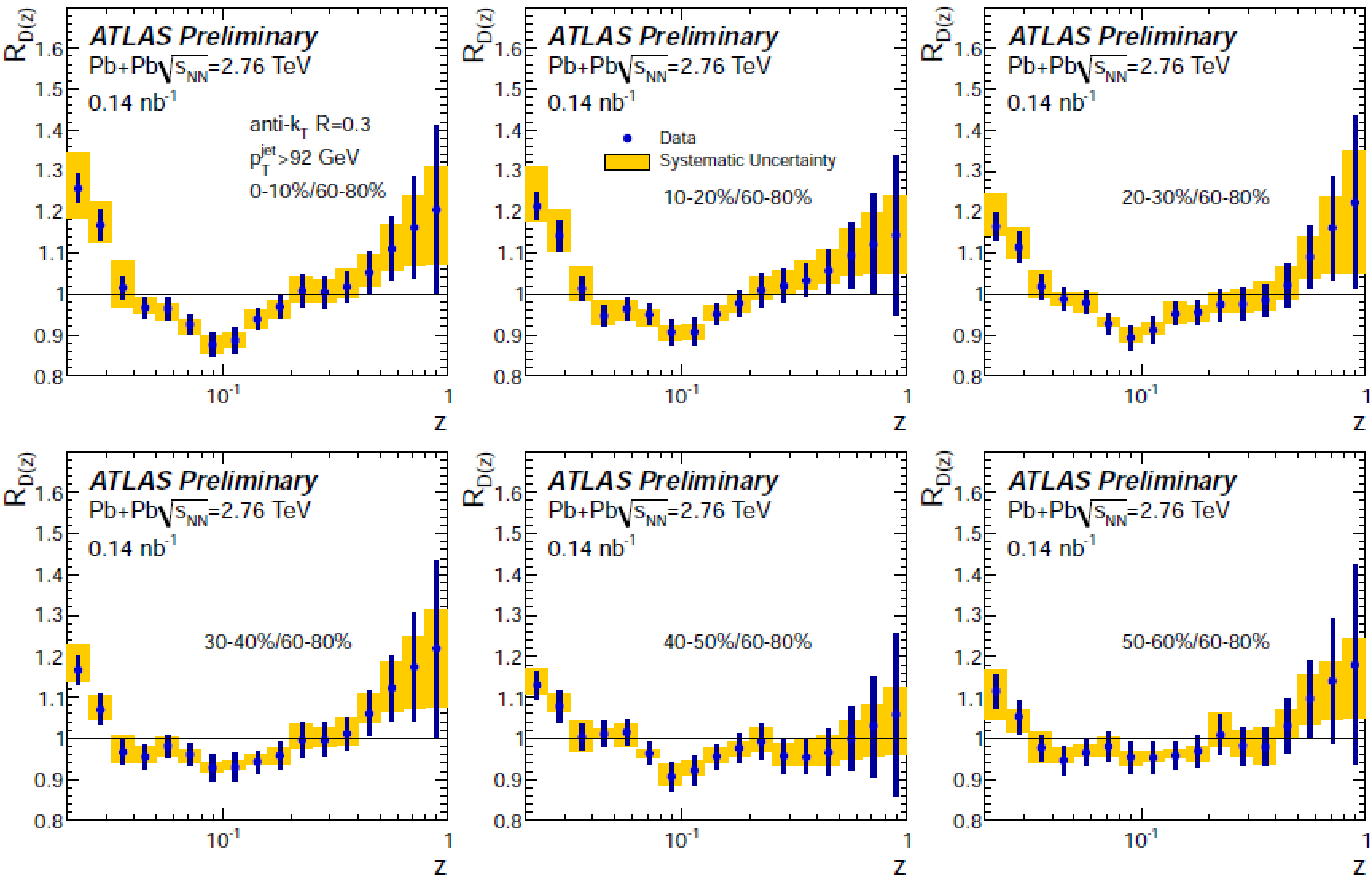
ATLAS Preliminary
Pb+Pb $\sqrt{s_{NN}}$=2.76 TeV
0.14 nb^{-1}
anti-k_T R=0.3
p_T^{jet}>92 GeV
0-10%/60-80%
Data
Systematic Uncertainty
10-20%/60-80%
20-30%/60-80%
30-40%/60-80%
40-50%/60-80%
50-60%/60-80%
$R_{D(z)}$
z
0.8
0.9
1
1.1
1.2
1.3
1.4
1.5
1.6
10^{-1}
1

$R_{D(z)}$ for R=0.2

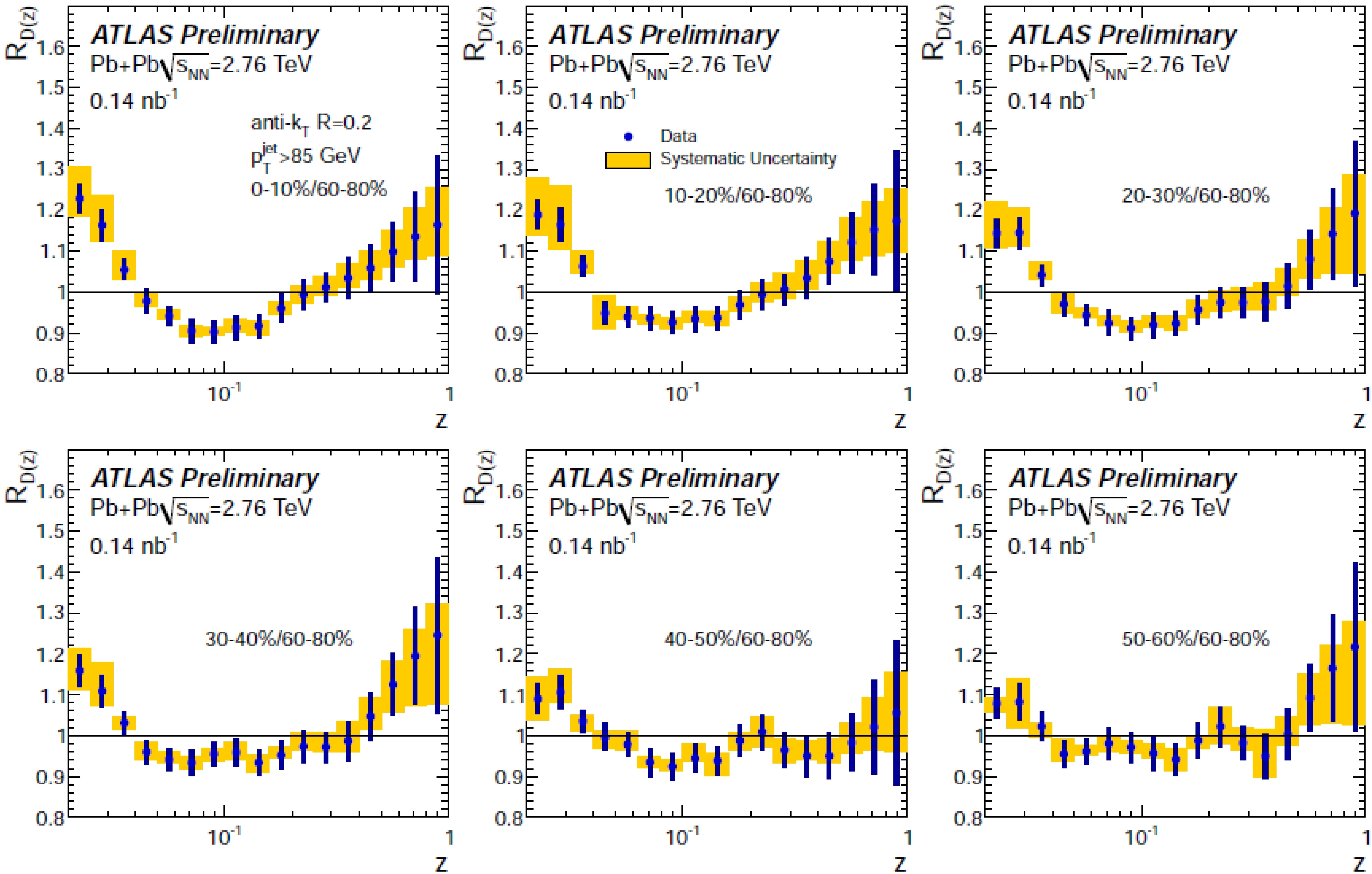

ATLAS Preliminary
Pb+Pb $\sqrt{s_{NN}}$=2.76 TeV
0.14 nb^{-1}
anti-k_T R=0.2
p_T^{jet}>85 GeV
0-10%/60-80%
Data
Systematic Uncertainty
10-20%/60-80%
20-30%/60-80%
30-40%/60-80%
40-50%/60-80%
50-60%/60-80%
$R_{D(z)}$
z

$R_{D(pt)}$ for R=0.3

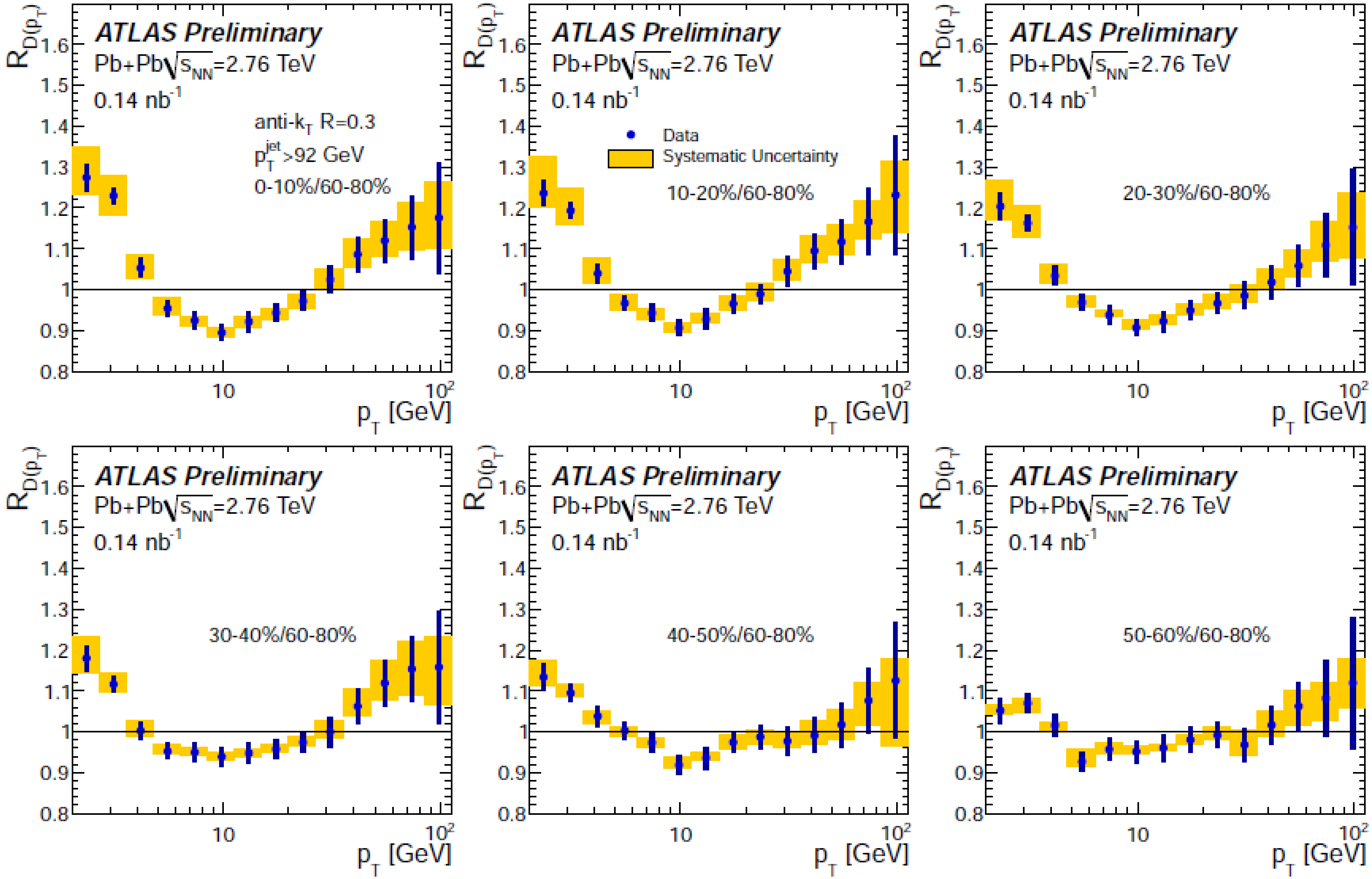
ATLAS Preliminary
Pb+Pb $\sqrt{s_{NN}}$=2.76 TeV
0.14 nb^{-1}
anti-k_T R=0.3
p_T^{jet}>92 GeV
0-10%/60-80%
Data
Systematic Uncertainty
10-20%/60-80%
20-30%/60-80%
30-40%/60-80%
40-50%/60-80%
50-60%/60-80%
$R_{D(p_T)}$
p_T [GeV]

$R_{D(pt)}$ for R=0.2

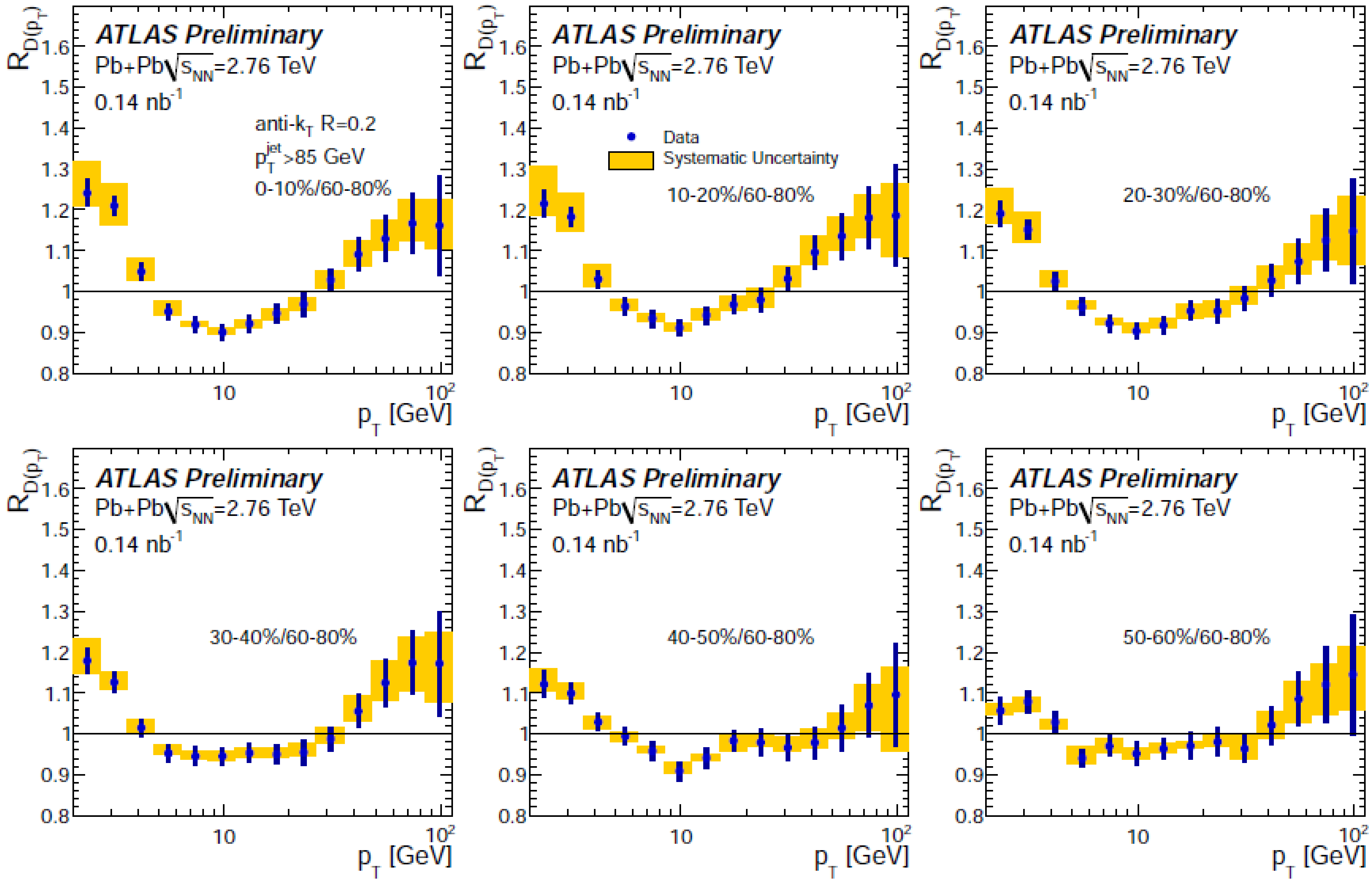
ATLAS Preliminary
Pb+Pb $\sqrt{s_{NN}}$=2.76 TeV
0.14 nb^{-1}
anti-k_T R=0.2
p_T^{jet}>85 GeV
0-10%/60-80%
Data
Systematic Uncertainty
10-20%/60-80%
20-30%/60-80%
30-40%/60-80%
40-50%/60-80%
50-60%/60-80%
$R_{D(p_T)}$
p_T [GeV]

Efficiency and bin-by-bin corrections for the neighboring jets

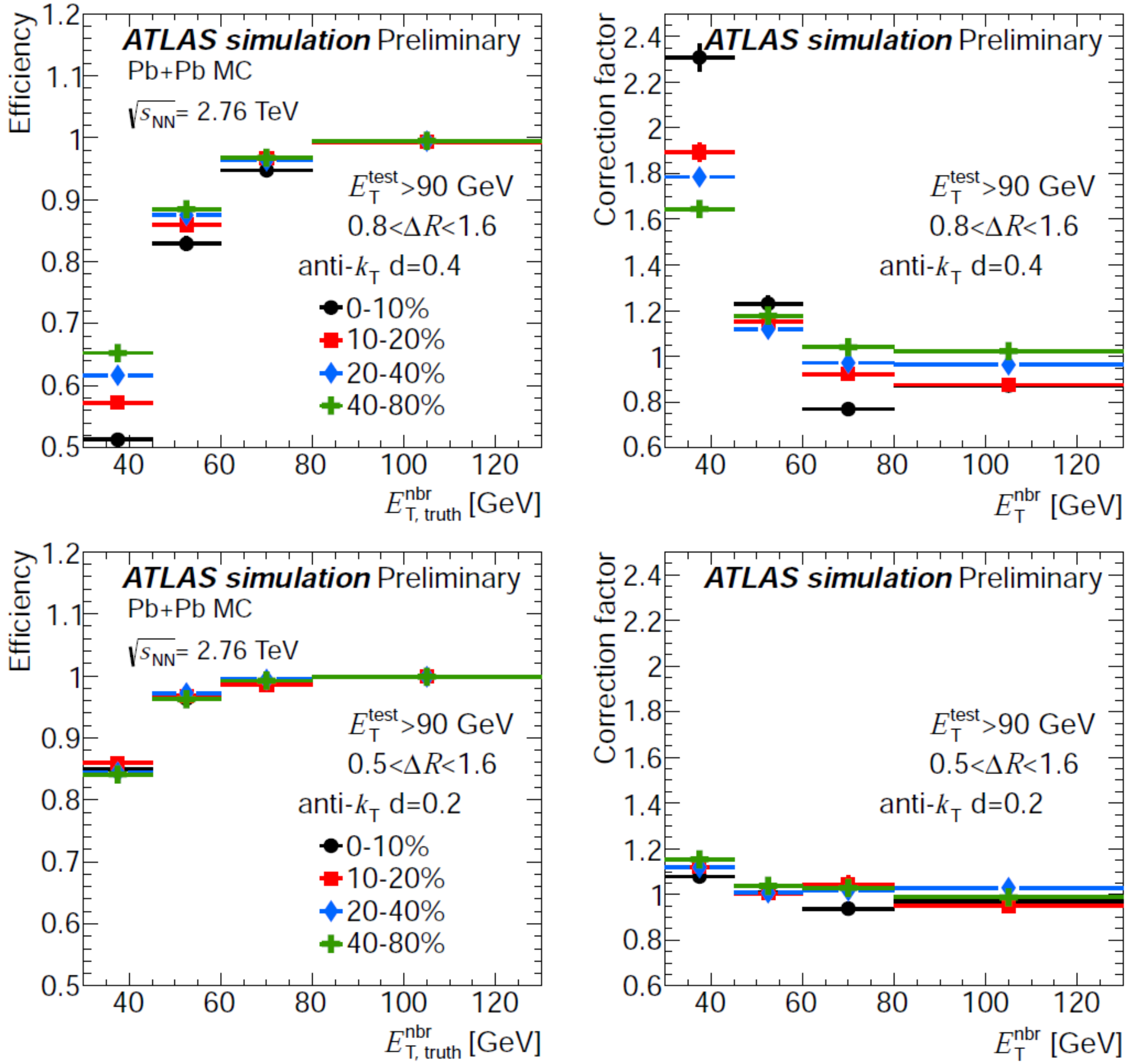

Systematic uncertainties for the neighboring jet measurement

	$\delta R_{\Delta R}$		$\delta\rho_{R_{\Delta R}}$
	0–10%	40–80%	0–10%
JES	12%	6%	5 %
JER	4%	2%	2%
Angular resolution	2%	0.5%	2%
Unfolding	6%	2%	5%
MC	5%	5%	5%
Trigger	5%	–	5%

Systematic uncertainties for the neighboring jet measurement

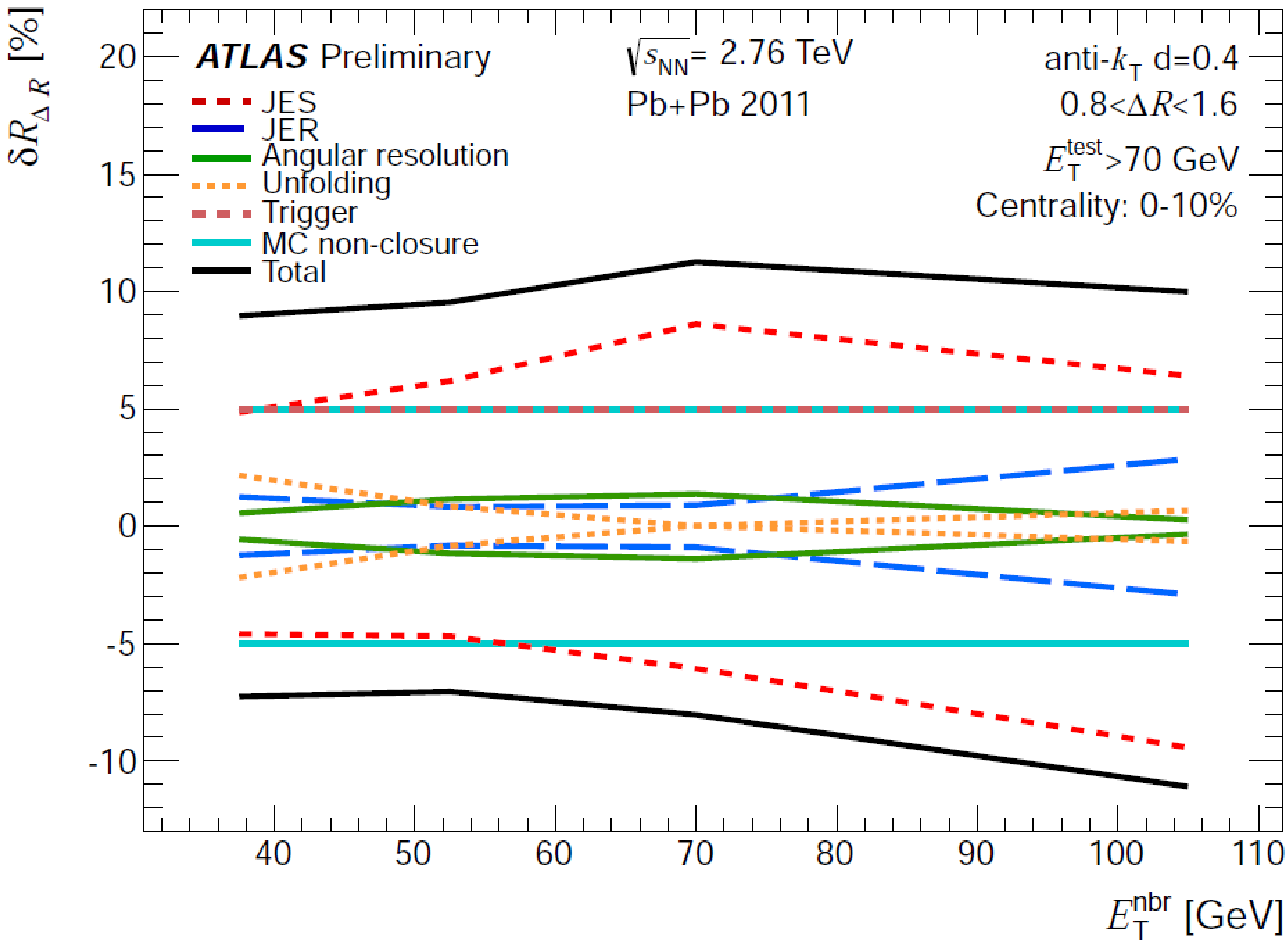

Systematic uncertainties for the neighboring jet measurement